INTERNATIONAL STANDARD

ISO 9300

Second edition
2005-08-15

Measurement of gas flow by means of critical flow Venturi nozzles

Mesure de débit de gaz au moyen de Venturi-tuyères en régime critique

Reference number
ISO 9300:2005(E)

PDF disclaimer

This PDF file may contain embedded typefaces. In accordance with Adobe's licensing policy, this file may be printed or viewed but shall not be edited unless the typefaces which are embedded are licensed to and installed on the computer performing the editing. In downloading this file, parties accept therein the responsibility of not infringing Adobe's licensing policy. The ISO Central Secretariat accepts no liability in this area.

Adobe is a trademark of Adobe Systems Incorporated.

Details of the software products used to create this PDF file can be found in the General Info relative to the file; the PDF-creation parameters were optimized for printing. Every care has been taken to ensure that the file is suitable for use by ISO member bodies. In the unlikely event that a problem relating to it is found, please inform the Central Secretariat at the address given below.

ISO copyright office
Case postale 56 • CH-1211 Geneva 20
Tel. + 41 22 749 01 11
Fax + 41 22 749 09 47
E-mail copyright@iso.org
Web www.iso.org

Published in Switzerland

Contents

Page

Foreword

ISO (the International Organization for Standardization) is a worldwide federation of national standards bodies (ISO member bodies). The work of preparing International Standards is normally carried out through ISO technical committees. Each member body interested in a subject for which a technical committee has been established has the right to be represented on that committee. International organizations, governmental and non-governmental, in liaison with ISO, also take part in the work. ISO collaborates closely with the International Electrotechnical Commission (IEC) on all matters of electrotechnical standardization.

International Standards are drafted in accordance with the rules given in the ISO/IEC Directives, Part 2.

The main task of technical committees is to prepare International Standards. Draft International Standards adopted by the technical committees are circulated to the member bodies for voting. Publication as an International Standard requires approval by at least 75 % of the member bodies casting a vote.

Attention is drawn to the possibility that some of the elements of this document may be the subject of patent rights. ISO shall not be held responsible for identifying any or all such patent rights.

ISO 9300 was prepared by Technical Committee ISO/TC 30, *Measurement of fluid flow in closed conduits*, Subcommittee SC 2, *Pressure differential devices*.

This second edition cancels and replaces the first edition (ISO 9300:1990), which has been technically revised.

Measurement of gas flow by means of critical flow Venturi nozzles

1 Scope

This International Standard specifies the geometry and method of use (installation in a system and operating conditions) of critical flow Venturi nozzles (CFVN) used to determine the mass flow-rate of a gas flowing through a system. It also gives the information necessary for calculating the flow-rate and its associated uncertainty.

It is applicable to Venturi nozzles in which the gas flow accelerates to the critical velocity at the throat (this being equal to the local sonic velocity), and only where there is steady flow of single-phase gases. At the critical velocity, the mass flow-rate of the gas flowing through the Venturi nozzle is the maximum possible for the existing upstream conditions while CFVN can only be used within specified limits, e.g. limits for the nozzle throat to inlet diameter ratio and throat Reynolds number. This International Standard deals with CFVN for which direct calibration experiments have been made in sufficient number to enable the resulting coefficients to be used with certain predictable limits of uncertainty.

Information is given for cases where the pipeline upstream of the CFVN is of circular cross-section, or it can be assumed that there is a large space upstream of the CFVN or upstream of a set of CFVN mounted in a cluster. The cluster configuration offers the possibility of installing CFVN in parallel, thereby achieving high flow-rates.

For high-accuracy measurement, accurately machined Venturi nozzles are described for low Reynolds number applications.

2 Terms and definitions

For the purposes of this document, the following terms and definitions apply.

2.1 Pressure measurement

2.1.1
wall pressure tapping
hole drilled in the wall of a conduit in such a way that the edge of the hole is flush with the internal surface of the conduit

NOTE The tapping is achieved such that the pressure within the hole is the static pressure at that point in the conduit.

2.1.2
static pressure of a gas
actual pressure of the flowing gas which can be measured by connecting a pressure gauge to a wall pressure tapping

NOTE Only the value of the absolute static pressure is used in this International Standard.

2.1.3
stagnation pressure
pressure which would exist in a gas in a flowing gas stream if the stream were brought to rest by an isentropic process

NOTE Only the value of the absolute stagnation pressure is used in this International Standard.

2.2 Temperature measurement

2.2.1
static temperature
actual temperature of a flowing gas

NOTE Only the value of the absolute static temperature is used in this International Standard.

2.2.2
stagnation temperature
temperature which would exist in a gas in a flowing gas stream if the stream were brought to rest by an isentropic process

NOTE Only the value of the absolute stagnation temperature is used in this International Standard.

2.3 Venturi nozzles

2.3.1
Venturi nozzle
convergent/divergent restriction inserted in a system intended for the measurement of flow-rate

2.3.2
normally machined Venturi nozzle
Venturi nozzle machined by a lathe and surface polished to achieve the desired smoothness

2.3.3
accurately machined Venturi nozzle
Venturi nozzle machined by a super-accurate lathe to achieve a mirror finish without polishing

2.3.4
throat
section of minimum diameter of a Venturi nozzle

2.3.5
critical flow Venturi nozzle
CFVN
Venturi nozzle for which the nozzle geometrical configuration and conditions of use are such that the flow-rate is critical at the nozzle throat

2.4 Flow

2.4.1
mass flow-rate
q_m
mass of gas per unit time passing through the CFVN

NOTE In this International Standard, the term flow-rate always refers to *mass flow-rate*.

2.4.2
throat Reynolds number
Re_{nt}
dimensionless parameter calculated from the gas flow-rate and the gas dynamic viscosity at nozzle inlet stagnation conditions

NOTE The characteristic dimension is taken as the throat diameter at stagnation conditions. The throat Reynolds number is given by the formula:

$$Re_{\mathrm{nt}} = \frac{4q_m}{\pi d \mu_0}$$

2.4.3
isentropic exponent
κ
ratio of the relative variation in pressure to the corresponding relative variation in density under elementary reversible adiabatic (isentropic) transformation conditions

NOTE 1 The isentropic exponent is given by the formula:

$$\kappa = \frac{\rho}{p}\left(\frac{\mathrm{d}p}{\mathrm{d}\rho}\right)_{\mathrm{s}} = \frac{\rho c^2}{p}$$

where

p is the absolute static pressure of the gas;

ρ is the density of the gas;

c is the local speed of sound;

s signifies “at constant entropy”.

NOTE 2 For an ideal gas, κ is equal to the ratio of specific heat capacities γ and is equal to 5/3 for monatomic gases, 7/5 for diatomic gases, 9/7 for triatomic gases, etc.

NOTE 3 In real gases, the forces exerted between molecules as well as the volume occupied by the molecules have a significant effect on the gas behaviour. In an ideal gas, intermolecular forces and the volume occupied by the molecules can be neglected.

2.4.4
discharge coefficient
C_{d}
dimensionless ratio of the actual flow-rate to the ideal flow-rate of non-viscous gas that would be obtained with one-dimensional isentropic flow for the same upstream stagnation conditions

NOTE This coefficient corrects for viscous and flow field curvature effects. For each type of nozzle design and installation conditions specified in this International Standard, it is only a function of the throat Reynolds number.

2.4.5
critical flow
maximum flow-rate for a particular Venturi nozzle, which can exist for the given upstream conditions

NOTE When critical flow exists, the throat velocity is equal to the local value of the speed of sound (acoustic velocity), the velocity at which small pressure disturbances propagate.

2.4.6
critical flow function
C^*
dimensionless function which characterises the thermodynamic flow properties of an isentropic and one-dimensional flow between the inlet and the throat of a Venturi nozzle

NOTE It is a function of the nature of the gas and of stagnation conditions (see 4.2).

2.4.7
real gas critical flow coefficient
C_{R}
alternative form of the critical flow function, more convenient for gas mixtures

NOTE It is related to the critical flow function as follows:

$$C_{\mathrm{R}} = C^* \sqrt{Z}$$

2.4.8
critical pressure ratio
r_*
ratio of the static pressure at the nozzle throat to the stagnation pressure for which the gas mass flow-rate through the nozzle is a maximum

NOTE This ratio is calculated in accordance with the equation given in 8.5.

2.4.9
back-pressure ratio
ratio of the nozzle exit static pressure to the nozzle upstream stagnation pressure

2.4.10
Mach number
Ma
⟨at nozzle upstream static conditions⟩ ratio of the mean axial fluid velocity to the velocity of sound at the location of the upstream pressure tapping

2.4.11
compressibility factor
Z
correction factor expressing numerically the deviation from the ideal gas law of the behaviour of a real gas at given pressure and temperature conditions

NOTE It is defined by the formula:

$$Z = \frac{pM}{\rho RT}$$

where R, the universal gas constant, equals 8,314 51 J/(mol·K).

2.5
uncertainty
parameter, associated with the results of a measurement, that characterizes the dispersion of the values that could reasonably be attributed to the measurand

3 Symbols

Symbol	Description	Dimension	SI unit
A_2	Cross-sectional area of Venturi nozzle exit	L^2	m^2
A_{nt}	Cross-sectional area of Venturi nozzle throat	L^2	m^2
$C_{d'}$	Coefficient of discharge	Dimensionless	
C_R	Critical flow coefficient for one-dimensional flow of a real gas	Dimensionless	
C_*	Critical flow function for one-dimensional flow of a real gas	Dimensionless	
C_{*i}	Critical flow function for one-dimensional isentropic flow of a perfect gas	Dimensionless	
D	Diameter of the upstream conduit	L	m
d	Diameter of Venturi nozzle throat	L	m
M	Molar mass	M	$kg\ mol^{-1}$
Ma_1	Mach number at the location of the upstream pressure tapping	Dimensionless	
p_1	Absolute static pressure of the gas at nozzle inlet	$ML^{-1}T^{-2}$	Pa
p_2	Absolute static pressure of the gas at nozzle exit	$ML^{-1}T^{-2}$	Pa
p_0	Absolute stagnation pressure of the gas at nozzle inlet	$ML^{-1}T^{-2}$	Pa
p_{nt}	Absolute static pressure of the gas at nozzle throat	$ML^{-1}T^{-2}$	Pa
p_{*i}	Absolute static pressure of the gas at nozzle throat for one-dimensional isentropic flow of a perfect gas	$ML^{-1}T^{-2}$	Pa
$(p_2/p_0)_i$	Ratio of nozzle exit static pressure to inlet stagnation pressure for one-dimensional isentropic flow of a perfect gas	Dimensionless	
q_m	Mass flow-rate	MT^{-1}	$kg{\cdot}s^{-1}$
q_{mi}	Mass flow-rate for one-dimensional isentropic flow of an inviscid gas	MT^{-1}	$kg{\cdot}s^{-1}$
R	Universal gas constant	$M\,L^2T^{-2}\Theta^{-1}$	$J{\cdot}mol^{-1}K^{-1}$
Re_{nt}	Nozzle throat Reynolds number	Dimensionless	
r_c	Radius of curvature of nozzle inlet	L	m
r_*	Critical pressure ratio p_{nt}/p_0	Dimensionless	
U'	Relative uncertainty	Dimensionless	
T_1	Absolute temperature of the gas at nozzle inlet	Θ	K
T_0	Absolute stagnation temperature of the gas at nozzle inlet	Θ	K
T_{nt}	Absolute static temperature at nozzle throat	Θ	K
v_{nt}	Throat sonic flow velocity; critical flow velocity at nozzle throat	LT^{-1}	$m{\cdot}s^{-1}$
Z	Compressibility factor	Dimensionless	
β	Diameter ratio d/D	Dimensionless	
γ	Ratio of specific heat capacities	Dimensionless	
δ	Absolute uncertainty	[a]	[a]
κ	Isentropic exponent	Dimensionless	
μ_0	Dynamic viscosity of the gas at stagnation conditions	$ML^{-1}T^{-1}$	Pa·s
μ_{nt}	Dynamic viscosity of the gas at nozzle throat	$ML^{-1}T^{-1}$	Pa·s
ρ_0	Gas density at stagnation conditions at nozzle inlet	ML^{-3}	$kg{\cdot}m^{-3}$
ρ_{nt}	Gas density at nozzle throat	ML^{-3}	$kg{\cdot}m^{-3}$

M = mass

L = length

T = time

Θ = temperature

[a] Same as the corresponding quantity.

4 Basic equations

4.1 State equation

The behaviour of a real gas can be described by the formula:

$$\frac{p}{\rho} = \left(\frac{R}{M}\right) TZ \tag{1}$$

4.2 Flow-rate under ideal conditions

For ideal critical flow to exist, three main conditions are necessary:

a) the flow must be one-dimensional;

b) the flow must be isentropic;

c) the gas must be perfect (i.e. $Z = 1$ and $\kappa = \gamma$).

Under these conditions, the critical flow-rate is given by:

$$q_{mi} = \frac{A_{\mathrm{nt}} C_{*i} p_0}{\sqrt{\left(\frac{R}{M}\right) T_0}} \tag{2}$$

or

$$q_{mi} = A_{\mathrm{nt}} C_{*i} \sqrt{p_0 \rho_0} \tag{3}$$

where

$$C_{*i} = \sqrt{\gamma \left(\frac{2}{\gamma + 1}\right)^{\frac{\gamma+1}{\gamma-1}}} \tag{4}$$

4.3 Flow-rate under real conditions

For flow-rates under real conditions, the formula for critical flow-rate becomes:

$$q_m = \frac{A_{\mathrm{nt}} C_{\mathrm{d}'} C_* p_0}{\sqrt{\left(\frac{R}{M}\right) T_0}} \tag{5}$$

or

$$q_m = A_{\mathrm{nt}} C_{\mathrm{d}'} C_{\mathrm{R}} \sqrt{p_0 \rho_0} \tag{6}$$

since

$$C_{\mathrm{R}} = C_* \sqrt{Z_0} \tag{7}$$

where Z_0 is the value of the compressibility factor at upstream stagnation conditions:

$$Z_0 = \frac{p_0 M}{\rho_0 R T_0} \tag{8}$$

It should be noted that C_* and C_R are not equal to C_{*i} because the gas is not perfect. $C_{d'}$ is less than unity since the flow is not one-dimensional and a boundary layer exists owing to viscous effects.

4.4 Critical mass flux

For the flow-rate under ideal conditions, critical mass flux $= \frac{q_{mi}}{A_{nt}}$

For the flow-rate under real conditions, critical mass flux $= \frac{q_m}{A_{nt} C_{d'}}$

5 Applications for which the method is suitable

Each application should be evaluated to determine whether a CFVN or some other device is the most suitable. An important consideration is that the flow through the Venturi nozzle is independent of the downstream pressure (see 9.5) within the pressure range for which the Venturi nozzle can be used for critical flow measurement.

Some other considerations are as follows.

For CFVN the only measurements required are the gas pressure and the gas temperature or density upstream of the critical Venturi nozzle, since the throat conditions can be calculated from thermodynamic considerations.

The velocity in the CFVN throat is the maximum possible for the given upstream stagnation conditions, and therefore the sensitivity to installation effects is minimized, except for those of swirl which shall not exist in the inlet part of the CFVN.

When comparing CFVN with subsonic pressure-difference meters, it can be noted that in the case of the CFVN, the flow is directly proportional to the nozzle upstream stagnation pressure and not, as in the case of the subsonic meter, to the square root of a measured differential pressure.

The maximum flow range which can be obtained for a given CFVN is generally limited to the range of inlet pressures which are available above the inlet pressure at which the flow becomes critical.

The most common applications to date for CFVN have been for tests, calibration and flow control.

6 Standard critical flow Venturi nozzles (CFVN)

6.1 General requirements

6.1.1 Materials

The CFVN shall be manufactured from material suitable for the intended application. Some considerations are that

a) it should be possible to finish the material to the required condition (as given in 6.1.2 and 6.1.3), taking into account that some materials are unsuitable owing to the inclusion of pits, voids and other inhomogeneities,

b) the material, together with any surface treatment used, shall not be subject to corrosion in the intended service, and

c) the material should be dimensionally stable and should have known and repeatable thermal expansion characteristics (if it is to be used at a temperature other than that at which the throat diameter has been measured), so that the appropriate throat diameter correction can be made.

6.1.2 Surface finish of the throat and the inlet

The throat and toroidal inlet up to the conical divergent section of the CFVN shall be smoothly finished so that the arithmetic average roughness Ra does not exceed $15 \times 10^{-6}\, d$ and 0,04 µm for normally and accurately machined Venturi nozzles, respectively.

The throat and toroidal inlet up the conical divergent section shall be free from dirt or any other contaminants.

For a normally machined CFVN, it is allowable to use a toroidal throat CFVN with a diameter step at the throat not larger than 10 % of the throat diameter.

6.1.3 Conical divergent

The form of the conical divergent section of the CFVN shall be checked to ensure that any steps, discontinuities, irregularities and lack of concentricity do not exceed 1 % of the local diameter. The arithmetic average roughness Ra of the conical divergent section shall not exceed $10^{-4}d$.

6.2 Design

6.2.1 General

There are two designs of standard CFVN: the toroidal-throat Venturi nozzle and the cylindrical throat Venturi nozzle. Accurately machined Venturi nozzles shall be built according to the toroidal design.

6.2.2 Toroidal-throat Venturi nozzle

6.2.2.1 The CFVN shall conform with the specifications shown in Figure 1.

6.2.2.2 For purposes of locating other elements of the CFVN metering system, the inlet plane of the CFVN is defined as that plane perpendicular to the axis of symmetry which intersects the inlet at a diameter equal to $2{,}5d \pm 0{,}1d$.

6.2.2.3 The convergent section of the CFVN nozzle (inlet) shall be a portion of a torus which shall extend from the inlet plane through the minimum area section (throat) and be tangential to the divergent section. The contour of the inlet upstream of the inlet plane (see 6.2.2.2) is not specified, except that the surface at each axial location shall have a diameter greater than or equal to the extension of the toroidal contour.

6.2.2.4 The toroidal surface of the CFVN located between the inlet plane and the divergent section (see Figure 1) shall not deviate from the shape of a torus by more than $\pm\, 0{,}001d$. The radius of curvature r_c of this toroidal surface in a plane in which the axis of symmetry lies shall be $1{,}8d$ to $2{,}2d$.

6.2.2.5 The divergent section of the CFVN downstream of the point of tangency with the torus shall form a frustum of a cone with a half-angle between 2,5° and 6°. The length of the divergent section shall be not less than the throat diameter.

6.2.2.6 The uncertainty in the measurement of flow-rate using CFVN built in accordance with this International Standard depends in particular on the uncertainly in the throat cross-sectional area. It is difficult to measure precisely the throat diameter of a toroidal throat CFVN, particularly in the case of small nozzles, and great care should be taken.

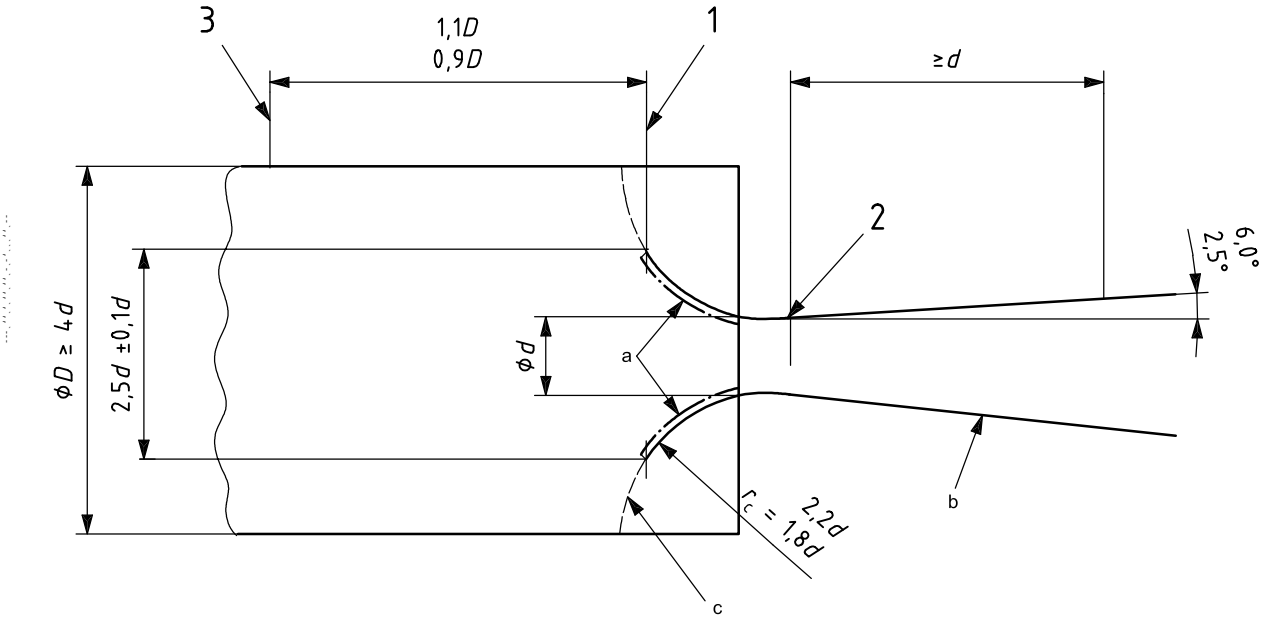

Key

1 inlet plane

2 intersection of toroidal surface and divergent section

3 location of pressure indicating device

a In this region the arithmetic average roughness Ra shall not exceed $15 \times 10^{-6}\, d$ and 0,04 µm for normally and accurately machined Venturi nozzles, respectively, and the contour shall not deviate from toroidal form by more than $\pm$ 0,001d.

b In this region the arithmetic roughness value shall not exceed $10^{-4}d$.

c Inlet surface shall lie outside this contour.

Figure 1 — Toroidal-throat Venturi nozzle

6.2.3 Cylindrical-throat Venturi nozzles

6.2.3.1 The CFVN shall conform with the specifications shown in Figure 2.

6.2.3.2 The inlet plane is defined as that plane which is tangential to the inlet contour of the CFVN and perpendicular to the nozzle centre-line.

6.2.3.3 The convergent section of the CFVN (inlet) shall be a quarter of a torus tangential on one hand to the inlet plane (see 6.2.3.2) and on the other hand to the cylindrical throat. The length of the cylindrical throat and the radius of curvature r_c of the quarter of torus shall be equal to the throat diameter.

6.2.3.4 The inlet toroidal surface of the CFVN shall not deviate from the shape of a torus by more than $\pm$ 0,001d.

6.2.3.5 The flow-rate shall be calculated from the mean diameter at the cylindrical throat outlet section. The mean diameter shall be determined by measuring at least four angularly equally distributed diameters on the cylindrical throat outlet. No diameter along the throat length shall deviate by more than $\pm$ 0,001d from the mean diameter.

The length of the throat shall not deviate from the throat diameter by more than 0,05d. The connection between the quarter of torus and the cylindrical throat shall be inspected visually and no defect should be observed. When a defect of connection is observed, it shall be checked that the local radius of curvature in a

plane in which the axis of symmetry lies is never less than 0,5d throughout the inlet surface (quarter of torus and cylindrical throat). Figure 3 illustrates this requirement.

The total area of the inlet and throat surfaces shall be properly polished so that the arithmetic average roughness Ra does not exceed $15 \times 10^{-6}\ d$.

The connection between the cylindrical throat and the divergent section shall also be visually inspected and no defect shall be observed.

6.2.3.6 The divergent section of the CFVN comprises a frustum of a cone with a half-angle between 3° and 4°. The length of the divergent section shall be not less than the throat diameter.

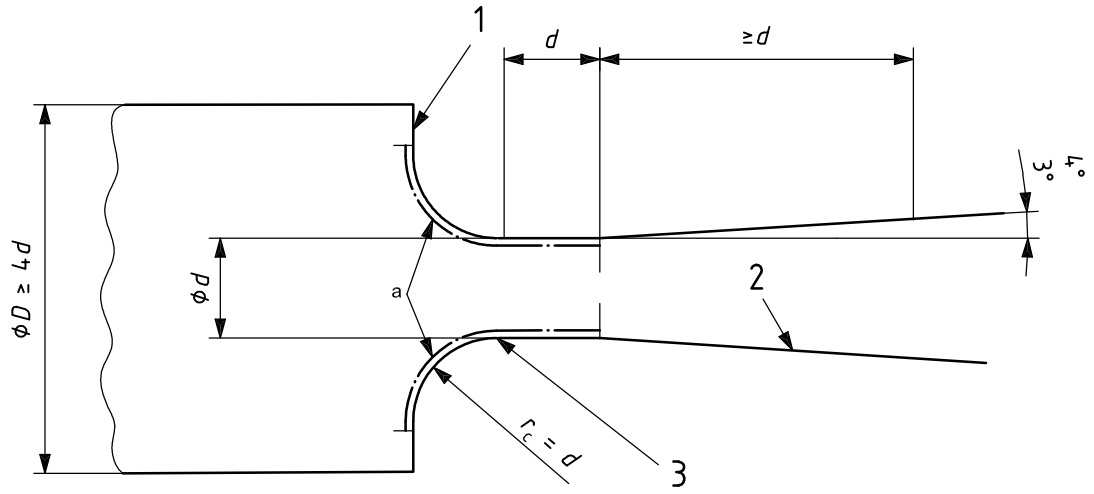

Key

1 inlet plane

2 conical divergent section with an arithmetic average relative roughness not exceeding $10^{-4}d$

3 transition region

a In this region the arithmetic average roughness Ra shall not exceed $15 \times 10^{-6}\ d$ and the contour shall not deviate from toroidal and cylindrical forms by more than $\pm$ 0,001d.

Figure 2 — Cylindrical-throat Venturi nozzle

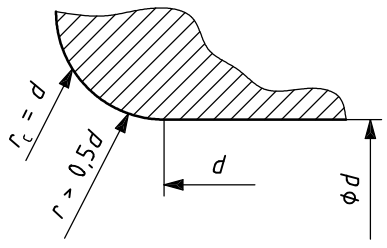

Figure 3 — Detail of connection between quarter of torus and cylindrical throat (transition region)

7 Installation requirements

7.1 General

This International Standard applies to the installation of CFVN when either

a) the pipeline upstream of the CFVN is of circular cross-section, or

b) it can be assumed that there is a large space upstream of the CFVN or a set of CFVN mounted in a cluster.

In the case of a), the CFVN shall be installed in a system meeting the requirements of 7.2.

In the case of b), the CFVN shall be installed in a system meeting the requirements of 7.3.

In either case, swirl shall not exist upstream of the CFVN. Where a pipeline exists upstream of the nozzle, swirl-free conditions can be ensured by installing a flow straightener of the design shown in Figure 4 at a distance $l_1 > 5D$ upstream of the nozzle inlet plane or any type of other flow conditioners of recognised type having equivalent or better performance — see [1] and [2] in the Bibliography.

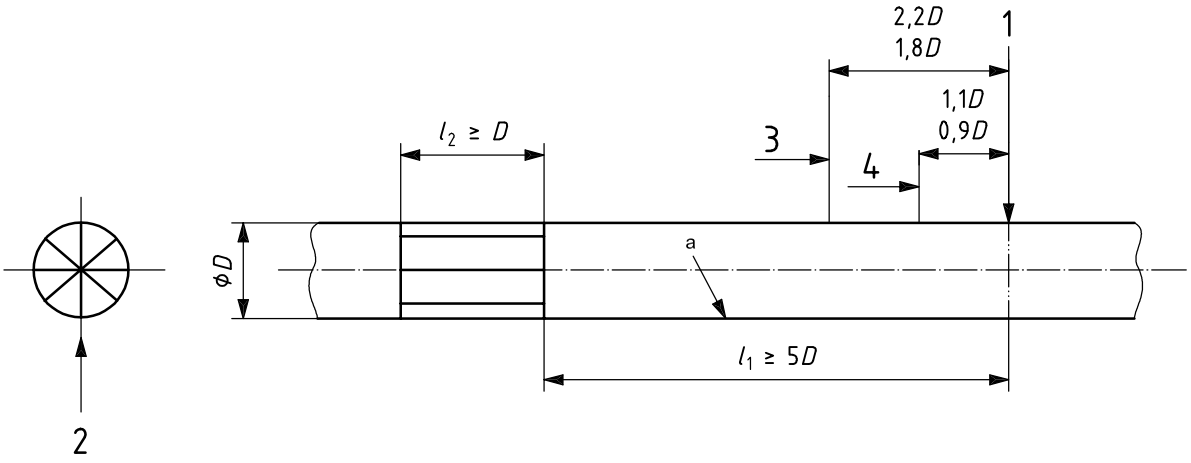

Key

1 inlet plane
2 etoile straightener with vane thickness adequate to prevent buckling
3 location of temperature sensor
4 location of pressure tapping

a In this region the surface roughness shall not exceed $10^{-4}D$.

Figure 4 — Installation requirements for upstream pipework configuration

7.2 Upstream pipeline

The primary device may be installed in a straight circular conduit which shall be concentric within $\pm$ 0,02D with the centre line of the CFVN. The inlet conduit up to 3D upstream of the CFVN shall not deviate from circularity by more than 0,01D and shall have an arithmetic average roughness Ra which shall not exceed $10^{-4}D$. The diameter of the inlet conduit shall be a minimum of 4d ($\beta \leqslant$ 0,25).

In cases where upstream installation constraints are such that the above requirement cannot be met, specific tests are recommended to investigate the influence of the installation conditions on the uncertainty of the flow-rate measurement and/or the determination of $C_{d'}$, when running a primary calibration. A correction method is given in this International Standard for the calculation of the mass flow-rate when $\beta >$ 0,25.

7.3 Large upstream space

It can be assumed that there is a large space upstream of the primary device if there is no wall closer than $5d$ to the axis of the primary device or to the inlet plane of the primary device, as defined in 6.2.2.2 or 6.2.3.2.

In cases of a large upstream space, or for high flow-rates, multiple CFVNs may be used.

7.4 Downstream requirements

No requirements are imposed on the outlet conduit except that it shall not restrict the flow in a manner such as to prevent critical flow in the CFVN.

7.5 Pressure measurement

7.5.1 When a circular conduit is used upstream of the primary device, the upstream static pressure shall preferably be measured at a wall pressure tapping at a distance $0{,}9D$ to $1{,}1D$ from the inlet plane of the Venturi nozzle (see Figures 1 and 4). The wall pressure tapping may be located upstream or downstream of this position, provided that it has been demonstrated that the measured pressure can be used reliably to give the nozzle inlet stagnation pressure.

7.5.2 When it can be assumed that there is a large space upstream of the primary device, the upstream wall pressure tapping shall preferably be located in a wall perpendicular to the inlet face of the primary device and within a distance of $10d \pm 1d$ from that plane. The wall pressure tapping may be located upstream or downstream of this position, provided that it has been demonstrated that the measured pressure can be used reliably to give the nozzle inlet stagnation pressure.

7.5.3 For the wall pressure tapping referred to in 7.5.1, and preferably also for that in 7.5.2, the centreline of the wall pressure tapping shall meet the centreline of the primary device and be at right angle to it. At the point of the breakthrough, the hole shall be circular. The edges shall be free from burrs, and shall be square or lightly rounded to a radius not exceeding 0,1 times the diameter of the wall pressure tapping. It shall be confirmed by visual inspection that the wall pressure tappings comply with these requirements. When an upstream pipeline is used, the diameter of the wall pressure tapping shall be less than $0{,}08D$ and less than 12 mm. The wall pressure tapping shall be cylindrical for a minimum length of 2,5 times the diameter of the tapping (see Figure 5).

Dimensions in millimetres

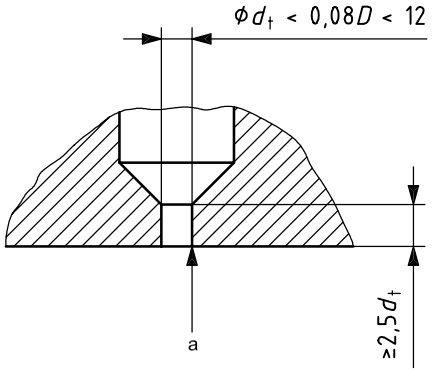

a Edge of hole flush with internal surface of conduit, burr-free and square to a radius not exceeding $0{,}1d_t$.

Figure 5 — Detail of wall pressure tapping when upstream pipeline is used

7.5.4 The downstream pressure shall be measured to ensure that critical flow is maintained. This pressure shall be measured by using a conduit wall pressure tapping located within 0,5 times the conduit diameter of the exit plane of the divergent section.

The critical flow may also be checked by measuring the wall pressure at the step located immediately downstream of the nozzle throat. That method requires special machining of the CFVN (see 6.1.3).

7.5.5 In some applications, the outlet pressure can be determined without the use of a wall pressure tapping. For example, the CFVN may discharge directly into the atmosphere or other region of known pressure. In these applications the outlet pressure need not be measured.

7.6 Drain holes

The conduit may be provided with the necessary drain holes for the removal of condensate or other foreign substances that may collect in some applications. There should be no flow through these drain holes while the flow measurement is in progress. If drain holes are required, they shall be located upstream of the nozzle upstream wall pressure tapping. The diameter of the drain holes should be smaller than $0{,}06D$. The axial distance from the drain hole to the plane of the upstream wall pressure tapping shall be greater than D and the hole shall be located in an axial plane different from that of the wall pressure tapping.

During measurement, flow must be single-phase upstream and in the throat with no condensation and all surfaces must retain their cleanliness and hence surface finish. If this cannot be guaranteed, the measurement shall not be claimed to conform to this International Standard.

7.7 Temperature measurement

The inlet temperature shall be measured using one or more sensors located upstream of the CFVN. When an upstream pipeline is used, the recommended location of these sensors is $1{,}8D$ to $2{,}2D$ upstream of the inlet plane of the CFVN. The diameter of the sensing element shall be not larger than $0{,}04D$ and the element shall not be aligned with a wall pressure tapping in the flow direction. If it is impracticable to use a sensing element of diameter less than $0{,}04D$, the sensing element shall be so located that it can be demonstrated that it does not affect the pressure measurement. The sensor may be located further still upstream, provided that it has been demonstrated that the measured temperature can be used reliably to give the nozzle inlet stagnation temperature.

Particular care has to be exercised in the selection of the temperature sensor and the insulation of pipework if the stagnation temperature of the flowing gas differs from that of the medium surrounding the pipeline by more than 5 K. In such cases, the sensor selected shall be insensitive to radiation error and the pipework shall be well lagged to minimize heat transfer between the flowing gas and the surrounding medium. If the temperatures of the flowing gas and the pipe wall differ significantly, it is extremely difficult to measure the gas temperature accurately.

7.8 Density measurement

For some applications, it may be desirable to measure directly the gas density at the nozzle inlet — for instance when the molar mass of the gas is not known with a sufficient accuracy.

When a densitometer is used, it shall be installed upstream of the nozzle and of the upstream pressure and temperature tappings. To achieve correct measurement of the inlet gas density, particular attention shall be given to the following points.

a) The installation of the densitometer shall not disturb the pressure and temperature measurements.

b) When the densitometer is located outside the main upstream pipe, checks shall be carried out to ensure that the gas in the device is the same as the gas flowing in the main conduit.

c) The pressure and temperature conditions at the densitometer should be as close as possible to the nozzle inlet conditions in order to avoid corrections. If necessary, the inlet density shall be computed from the measured density using the equation of state:

$$\rho_0 = \rho_{\text{den}} \frac{p_0 T_{\text{den}} Z_{\text{den}}}{p_{\text{den}} T_0 Z_0} \tag{9}$$

where

den as a subscript signifies “relative to the densitometer”;

T_{den} is the temperature that should be measured;

p_{den} is the pressure that should be determined by measurement of the difference from p_0;

Z_{den}/Z_0 is calculated using the specifications of 7.9.

7.9 Calculated density

Instead of the measurement of the density, a calculation may be performed using the gas composition determined by gas chromatography, combined with a recognised equation such as the one proposed by ISO 6976:1995 [3] in particular. The uncertainty of the method is as good as the uncertainty obtained with a densitometer.

8 Calculation methods

8.1 Mass flow-rate

The actual mass flow-rate shall be computed from one of the following equations:

$$q_m = \frac{A_{nt} C_{d'} C_* p_0}{\sqrt{\left(\frac{R}{M}\right) T_0}}$$

or

$$q_m = A_{nt} C_{d'} C_R \sqrt{p_0 \rho_0}$$

where A_{nt} is calculated from the value of d.

8.2 Discharge coefficient, $C_{d'}$

8.2.1 The discharge coefficient depends largely on the shape of the CFVN and it shall be noted that at small values of the throat diameter the nozzle geometry is very difficult to control and measure (see 6.2.2.6).

8.2.2 The discharge coefficient for the CFVN may be obtained from the following equation:

$$C_{d'} = a - bRe_{nt}^{-n} \tag{10}$$

The coefficients a, b and n are given in Table 1 for each type of CFVN for the range of throat Reynolds number over which they may be used.

Table 1 — Coefficients a, b and n

Toroidal-throat Venturi nozzle	
$2{,}1 \times 10^4 < Re_{nt} < 3{,}2 \times 10^7$	$a = 0{,}995\ 9$ $b = 2{,}720$ $n = +0{,}5$
Accurately machined toroidal-throat Venturi nozzle	
$2{,}1 \times 10^4 < Re_{nt} < 1{,}4 \times 10^6$	$a = 0{,}998\ 5$ $b = 3{,}412$ $n = +0{,}5$
Cylindrical-throat Venturi nozzle	
$3{,}5 \times 10^5 < Re_{nt} < 1{,}1 \times 10^7$	$a = 0{,}997\ 6$ $b = 0{,}138\ 8$ $n = +0{,}2$

8.2.3 The relative uncertainty in the discharge coefficients obtained from Equation (10) is 0,3 %, at the 95 % confidence level, for the toroidal-throat and cylindrical-throat Venturi nozzles. For the accurately machined nozzle, this relative uncertainty in the discharge coefficients is 0,2 % at the 95 % confidence level.

Values of the discharge coefficient are given in Annex A.

8.3 Critical flow function, C_*, and real gas critical flow coefficient, C_R

The value of C_* used to calculate the gas mass flow-rate may be computed using any method of demonstrable accuracy.

Values of C_* for various gases are given in Annex B. The relative uncertainty in C_* obtained from Annex B is 0,1 % at the 95 % confidence level.

An applicable method to calculate C_* and thus C_R for natural gases uses AGA Report No. 8 (1992) [4] as the state equation. This approach ensures a relative uncertainty on C_* of 0,05 % at 95 % confidence level. Alternatively, any other state equation with comparable uncertainty can be used.

A method of computation of C_* for natural gas mixtures is given in Annex C from the calculation of the critical mass flux. The relative uncertainty in $q_m/(A_{nt}C_{d'})$ obtained from Annex C is 0,1 % at the 95 % confidence level.

8.4 Conversion of measured pressure and temperature to stagnation conditions

The inlet stagnation pressure, p_0, may be determined from the relationship:

$$\frac{p_0}{p_1} = \left[1 + \frac{1}{2}(\kappa - 1)Ma_1^2\right]^{\kappa/(\kappa-1)} \tag{11}$$

The inlet stagnation temperature, T_0, may be determined from the formula:

$$\frac{T_0}{T_1} = 1 + \frac{1}{2}(\kappa - 1)Ma_1^2 \tag{12}$$

The error in assuming the measurement temperature equals the stagnation temperature is negligible as long as the ratio d/D is $\leqslant$ 0,25 (see 7.2).

8.5 Maximum permissible downstream pressure

For CFVN operating at throat Reynolds numbers greater than 2×10^5 and having exit cones longer than d, the maximum permissible downstream pressure is determined from the relationship:

$$\left(\frac{p_2}{p_0}\right)_{\max} = 0{,}8\left[\left(\frac{p_2}{p_0}\right)_i - r_*\right] + r_* \tag{13}$$

where

$$r_* = \left(\frac{2}{\kappa+1}\right)^{\kappa/(\kappa-1)} \tag{14}$$

where κ should be determined from an appropriate equation of state.

The value of $(p_2/p_0)_i$ is determined from the isentropic ideal gas relationships as a function of the area ratio of the divergent section. Values of $(p_2/p_0)_{\max}$ may be determined from Figure 6. Higher back-pressure ratios than those shown may be used provided that it can be verified that the flow is critical. The pressure ratio $(p_2/p_o)_{\max}$ is not significantly affected by extending the cone length such that the exit area is greater than four times the throat area, i.e. diffuser length beyond seven diameters for a cone half-angle of 4°.

Pressure ratios of 0,95 are obtained with a very carefully machined throat and divergent section.

For CFVN operating at throat Reynolds numbers lower than 2×10^5, it is recommended that users maintain a back-pressure ratio of 0,25 or perform a simple unchoking test on their CFVNs [5].

Figure 6 is applicable to Reynolds numbers greater than 2×10^5.

The area ratio A_2/A_{nt} is related to the Venturi nozzle dimensions by the following formulae:

— For toroidal-throat Venturi nozzles:

$$\frac{A_2}{A_{\text{nt}}} = \left[\frac{2l\tan\theta}{d} + \frac{2r_{\text{c}}}{d}(1-\cos\theta) + 1\right]^2$$

— For cylindrical-throat Venturi nozzles:

$$\frac{A_2}{A_{\text{nt}}} = \left(\frac{2l\tan\theta}{d} + 1\right)^2$$

where

l is the length of the divergent section;

θ is the half-angle of the divergent section.

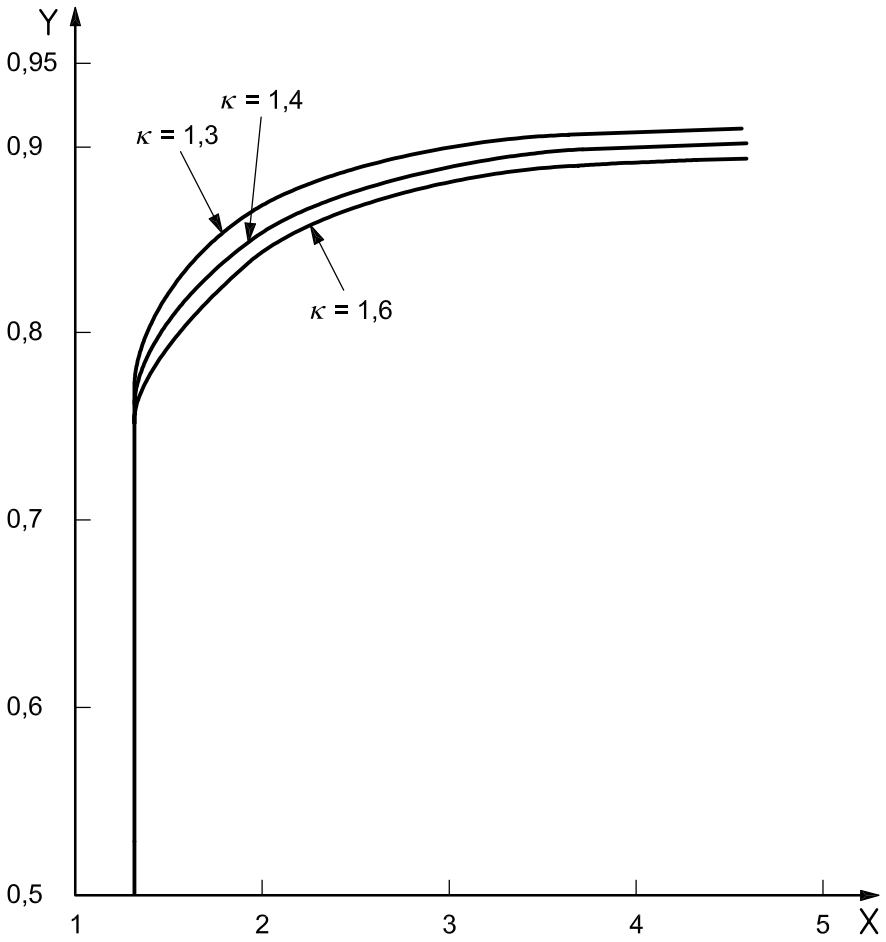

Key

X divergent cone area ratio, A_2/A_{nt}

Y maximum permissible back-pressure ratio $(p_2/p_0)_{max}$

Figure 6 — Maximum permissible back-pressure ratio for CFVN

9 Uncertainties in the measurement of flow-rate

9.1 General

9.1.1 Useful general information on this subject is given in [6].

9.1.2 The uncertainty in the measurement of the flow-rate shall be calculated and shall be reported as such whenever a measurement is claimed to be in conformity with this International Standard.

9.1.3 The uncertainty may be expressed in absolute or relative terms and the results of the flow measurement may then be given in any one of the following forms:

— rate of flow = $q_m \pm \delta q_m$

— rate of flow = $q_m[1 \pm U'(q_m)]$

— rate of flow = q_m within $[100U'(q_m)]$ %

where the absolute uncertainty δq_m shall have the same dimensions as q_m, and the relative uncertainty $U'(q_m)] = \delta q_m/q_m$ is non-dimensional.

9.1.4 The uncertainty in the flow measurement is equivalent to twice the standard deviation. As for the standard deviation, the uncertainty is obtained by combining the partial uncertainties of the individual quantities used in the calculation of the flow-rate — assuming them to be small, numerous and independent of one another. Although for a single measuring device, and for the coefficients used in one test, some of these uncertainties may in reality be systematic errors (of which only an estimation of their maximum absolute amount is known), their combination is permitted as if they were random uncertainties.

9.2 Practical computation of uncertainty

9.2.1 The basic formula for the computation of the mass rate of flow q_m is either

$$q_{\mathrm{m}} = \frac{A_{\mathrm{nt}} C_{\mathrm{d}'} C_* p_0}{\sqrt{\left(\frac{R}{M}\right) T_0}}$$

or

$$q_m = A_{\mathrm{nt}} C_{\mathrm{d}'} C_{\mathrm{R}} \sqrt{p_0 \rho_0}$$

In fact, the various quantities which appear on the right-hand side of these formulae are not independent and so it is not strictly correct to compute the uncertainty in q_m directly from the uncertainties in these quantities. (For example, C_* and C_{R} are functions of p_0 and T_0, and $C_{\mathrm{d}'}$ is a function of d, μ_0 and q_m.)

However, it is sufficient for most practical purposes to assume that the uncertainties in the terms on the right-hand side of the equations are independent of one another.

9.2.2 The practical working formula for calculating the relative uncertainty in the mass flow-rate q_m is

$$U'(q_m) = \sqrt{U'^2(C_{\mathrm{d}'}) + U'^2(C_*) + U'^2(A_{\mathrm{nt}}) + U'^2(p_0) + \frac{1}{4}U'^2(M) + \frac{1}{4}U'^2(T_0)} \tag{15}$$

or

$$U'(q_m) = \sqrt{U'^2(C_{\mathrm{d}'}) + U'^2(C_{\mathrm{R}}) + U'^2(A_{\mathrm{nt}}) + \frac{1}{4}U'^2(\rho_0) + \frac{1}{4}U'^2(p_0)} \tag{16}$$

When the inlet gas density is not directly measured but is computed from Equation (9), the uncertainty relative to ρ_0 is given by:

$$U'(\rho_0) = \left\{ \begin{array}{l} U'^2(\rho_{\mathrm{nt}}) + \left[1 - \left(\frac{\partial Z}{\partial p}\right)_{\mathrm{nt}} \left(\frac{p_{\mathrm{nt}}}{Z_{\mathrm{nt}}}\right)\right]^2 U'^2(p_{\mathrm{nt}}) \\ + \left[1 - \left(\frac{\partial Z}{\partial p}\right)_0 \left(\frac{p_0}{Z_0}\right)\right]^2 U'^2(p_0) \\ + \left[1 + \left(\frac{\partial Z}{\partial T}\right)_0 \left(\frac{T_0}{Z_0}\right)\right]^2 U'^2(T_0) \\ + \left[1 + \left(\frac{\partial Z}{\partial T}\right)_{\mathrm{nt}} \left(\frac{T_{\mathrm{nt}}}{Z_{\mathrm{nt}}}\right)\right]^2 U'^2(T_{\mathrm{nt}}) \end{array} \right\}^{1/2} \tag{17}$$

This often simplifies to:

$$U'(\rho_0) = \sqrt{U'^2(\rho_{\mathrm{nt}}) + U'^2(p_{\mathrm{nt}}) + U'^2(p_0) + U'^2(T_0) + U'^2(T_{\mathrm{nt}})} \tag{18}$$

Annex A
(normative)

Venturi nozzle discharge coefficients

Table A.1 gives the discharge coefficients at different Reynolds numbers at the nozzle throat for toroidal-throat Venturi nozzles.

Table A.1 — Discharge coefficients for toroidal-throat Venturi nozzles

Reynolds number Re_{nt}	Discharge coefficient $C_{d'}$
$2{,}1 \times 10^4$	0,977 1
3×10^4	0,980 2
5×10^4	0,983 7
7×10^4	0,985 6
1×10^5	0,987 3
2×10^5	0,989 8
3×10^5	0,990 9
5×10^5	0,992 1
7×10^5	0,992 6
1×10^6	0,993 2
3×10^6	0,994 3
7×10^6	0,994 9
1×10^7	0,995 0
$3{,}2 \times 10^7$	0,995 4

Table A.2 gives the discharge coefficients at different Reynolds numbers at the nozzle throat for accurately machined toroidal-throat Venturi nozzles.

Table A.2 — Discharge coefficients for accurately machined toroidal-throat Venturi nozzles

Reynolds number Re_{nt}	Discharge coefficient $C_{d'}$
$2{,}1 \times 10^4$	0,975 0
3×10^4	0,978 8
5×10^4	0,983 2
7×10^4	0,985 6
1×10^5	0,987 7
2×10^5	0,990 9
3×10^5	0,992 3
5×10^5	0,993 7
7×10^5	0,994 4
$1{,}4 \times 10^6$	0,995 6

Table A.3 gives the discharge coefficients at different Reynolds numbers at the nozzle throat for cylindrical-throat Venturi nozzles.

Table A.3 — Discharge coefficients for cylindrical-throat Venturi nozzles

Reynolds number Re_{nt}	Discharge coefficient $C_{d'}$
$3{,}5 \times 10^5$	0,989 8
5×10^5	0,990 9
7×10^5	0,992 1
1×10^6	0,992 6
3×10^6	0,993 2
7×10^6	0,994 3
$1{,}1 \times 10^7$	0,995 4

Annex B
(normative)

Tables of values for critical flow function C_* — Various gases

B.1 General

This annex provides the information necessary for calculating the critical flow function for several pure gases and dry air. Where possible, the values have been updated from the previous edition of ISO 9300 to make use of more recent reference quality equations of state; where no new work has been undertaken, the information remains unchanged. For some gases there are two methods for obtaining C_*: a table of values and an empirical equation. All of the information given here is traceable through the corresponding numbered bibliographical references.

B.2 Tables

C_* values are given in Tables B.1, B.3, B.5, B.7, B.9, B.10 and B.11 for nitrogen, argon, dry CO_2-free air, methane, carbon dioxide, oxygen and steam. These values are based on the best available thermodynamic data for each gas. The temperature (K) and pressure (MPa) are taken as the stagnation values.

B.3 Empirical equation

With the exception of carbon dioxide, oxygen and steam, an empirical equation has been developed to accurately represent the C_* values, removing the need for interpolation [7]. The equation is applicable over restricted temperature ranges. The empirical equation takes the form:

$$C_* = \sum_i a_i \pi^{b_i} \tau^{c_i} \tag{B.1}$$

where $\pi = \frac{p_0}{p_c}$ and $\tau = \frac{T_0}{T_c}$

The coefficients for this equation, and the corresponding critical parameters, are given separately for each gas underneath the relevant table of values. The use of this equation does not introduce any significant additional uncertainty into the critical flow calculation. Within the applicable temperature ranges, as given below, the use of this equation is recommended instead of interpolating from the tables.

B.4 Atmospheric air

The C_* values given in Table B.5 for dry air [or calculated from Equation (B.1) using the coefficients given in Table B.6 for dry air] are valid only for dry CO_2-free air. When a nozzle is used with atmospheric air that has not been dried, the mass flow-rate can be significantly affected. In such circumstances, users should apply the mass flow correction factor given in Annex D.

B.5 Nozzle throat to pipe diameter ratio, β

The values provided in this annex apply to cases where $\beta < 0{,}25$. If this condition is not met, there will be a small but significant velocity at the upstream measurement point. In such circumstances, the user should also apply the mass flow correction factor given in Annex E.

B.6 C_* values and coefficients for Equation (B.1)

Table B.1 gives values of C_* and Table B.2 coefficients for Equation (B.1) for nitrogen.

Table B.1 — C_* values — Nitrogen

T_0 K	p_0 MPa										
	0,1	**2**	**4**	**6**	**8**	**10**	**12**	**14**	**16**	**18**	**20**
200	0,685 61	0,703 67	0,724 97	0,748 45	0,773 43	0,798 56	0,822 04	0,842 30	0,858 42	0,870 23	0,878 09
220	0,685 38	0,698 67	0,713 60	0,729 28	0,745 30	0,761 09	0,775 99	0,789 38	0,800 81	0,810 06	0,817 10
240	0,685 22	0,695 21	0,706 08	0,717 14	0,728 16	0,738 84	0,748 89	0,758 03	0,766 04	0,772 80	0,778 25
260	0,685 10	0,692 72	0,700 83	0,708 90	0,716 79	0,724 34	0,731 40	0,737 82	0,743 52	0,748 40	0,752 44
280	0,685 00	0,690 88	0,697 02	0,703 03	0,708 82	0,714 30	0,719 38	0,723 99	0,728 08	0,731 60	0,734 55
300	0,684 92	0,689 48	0,694 17	0,698 70	0,703 00	0,707 03	0,710 74	0,714 08	0,717 03	0,719 56	0,721 68
320	0,684 85	0,688 39	0,691 98	0,695 40	0,698 62	0,701 60	0,704 31	0,706 73	0,708 85	0,710 65	0,712 13
340	0,684 78	0,687 52	0,690 26	0,692 85	0,695 24	0,697 44	0,699 41	0,701 14	0,702 63	0,703 87	0,704 86
360	0,684 70	0,686 81	0,688 89	0,690 82	0,692 58	0,694 17	0,695 58	0,696 79	0,697 80	0,698 61	0,699 22
380	0,684 62	0,686 21	0,687 76	0,689 18	0,690 45	0,691 57	0,692 53	0,693 33	0,693 97	0,694 44	0,694 75
400	0,684 52	0,685 70	0,686 82	0,687 83	0,688 71	0,689 45	0,690 07	0,690 54	0,690 88	0,691 09	0,691 16
420	0,684 41	0,685 25	0,686 03	0,686 70	0,687 26	0,687 71	0,688 04	0,688 26	0,688 36	0,688 35	0,688 24
440	0,684 28	0,684 84	0,685 33	0,685 73	0,686 04	0,686 24	0,686 35	0,686 36	0,686 27	0,686 09	0,685 82
460	0,684 13	0,684 45	0,684 71	0,684 89	0,684 98	0,684 99	0,684 91	0,684 75	0,684 51	0,684 19	0,683 79
480	0,683 95	0,684 09	0,684 15	0,684 15	0,684 07	0,683 91	0,683 68	0,683 38	0,683 01	0,682 58	0,682 07
500	0,683 76	0,683 73	0,683 64	0,683 48	0,683 25	0,682 96	0,682 61	0,682 20	0,681 72	0,681 19	0,680 60
520	0,683 55	0,683 38	0,683 15	0,682 86	0,682 52	0,682 12	0,681 66	0,681 15	0,680 59	0,679 98	0,679 32
540	0,683 31	0,683 03	0,682 69	0,682 29	0,681 85	0,681 35	0,680 81	0,680 22	0,679 59	0,678 92	0,678 20
560	0,683 05	0,682 68	0,682 24	0,681 75	0,681 22	0,680 65	0,680 04	0,679 39	0,678 70	0,677 97	0,677 21
580	0,682 78	0,682 32	0,681 80	0,681 24	0,680 64	0,680 01	0,679 34	0,678 63	0,677 89	0,677 12	0,676 32
600	0,682 49	0,681 96	0,681 38	0,680 75	0,680 10	0,679 41	0,678 68	0,677 93	0,677 15	0,676 35	0,675 51

Table B.2 — Coefficients for Equation (B.1) — Nitrogen

i	a_i	b_i	c_i
1	$5{,}205\ 142\ 20 \times 10^{-3}$	0	−4
2	$6{,}814\ 027\ 97 \times 10^{-1}$	0	0
3	$2{,}377\ 461\ 61 \times 10^{-3}$	0	1
4	$-4{,}519\ 510\ 40 \times 10^{-4}$	0	2
5	$-1{,}374\ 006\ 43 \times 10^{-1}$	1	−7
6	$1{,}499\ 853\ 26 \times 10^{-1}$	1	−3
7	$-2{,}290\ 164\ 23 \times 10^{-3}$	1	0
8	$3{,}299\ 637\ 65 \times 10^{-8}$	1	5
9	$-2{,}026\ 516\ 12 \times 10^{-3}$	1,5	−1
10	$3{,}024\ 106\ 16 \times 10^{-4}$	1,5	0
11	$2{,}837\ 231\ 67 \times 10^{-1}$	2,5	−8
12	$-1{,}129\ 149\ 85 \times 10^{-1}$	3	−8
13	$-2{,}531\ 933\ 90 \times 10^{-3}$	3	−4
14	$2{,}222\ 006\ 17 \times 10^{-5}$	3,5	−2
15	$1{,}190\ 308\ 45 \times 10^{-3}$	4	−6

Critical parameters:

$p_c = 3{,}395\ 8$ MPa

$T_c = 126{,}192$ K

For nitrogen, Equation (B.1) is valid over the temperature range 250 to 600 K at pressures up to 20 MPa. See [7] and [8].

Table B.3 gives values of C_* and Table B.4 coefficients for Equation (B.1) for argon.

Table B.3 — C_* values — Argon

T_0 K	p_0 MPa										
	0,1	**2**	**4**	**6**	**8**	**10**	**12**	**14**	**16**	**18**	**20**
200	—	—	—	—	—	—	—	—	—	—	—
220	0,727 19	0,747 57	0,771 78	0,799 09	0,829 51	0,862 53	0,896 82	0,930 35	0,960 92	0,986 87	1,007 46
240	0,726 98	0,742 75	0,760 74	0,780 16	0,800 86	0,822 48	0,844 48	0,866 12	0,886 59	0,905 15	0,921 29
260	0,726 82	0,739 26	0,753 08	0,767 56	0,782 56	0,797 87	0,813 20	0,828 21	0,842 53	0,855 83	0,867 83
280	0,726 70	0,736 67	0,747 52	0,758 66	0,769 98	0,781 35	0,792 61	0,803 55	0,814 01	0,823 82	0,832 81
300	0,726 60	0,734 69	0,743 35	0,752 11	0,760 90	0,769 61	0,778 16	0,786 43	0,794 32	0,801 74	0,808 60
320	0,726 53	0,733 14	0,740 15	0,747 15	0,754 09	0,760 92	0,767 57	0,773 97	0,780 06	0,785 79	0,791 11
340	0,726 47	0,731 92	0,737 64	0,743 30	0,748 86	0,754 30	0,759 55	0,764 59	0,769 37	0,773 87	0,778 04
360	0,726 42	0,730 94	0,735 63	0,740 25	0,744 76	0,749 13	0,753 33	0,757 34	0,761 14	0,764 70	0,768 01
380	0,726 38	0,730 14	0,734 02	0,737 80	0,741 48	0,745 02	0,748 41	0,751 63	0,754 67	0,757 51	0,760 14
400	0,726 35	0,729 48	0,732 69	0,735 81	0,738 82	0,741 70	0,744 45	0,747 04	0,749 48	0,751 76	0,753 85
420	0,726 32	0,728 93	0,731 60	0,734 17	0,736 64	0,738 99	0,741 22	0,743 31	0,745 27	0,747 09	0,748 76
440	0,726 30	0,728 48	0,730 69	0,732 81	0,734 83	0,736 74	0,738 55	0,740 24	0,741 81	0,743 26	0,744 59
460	0,726 28	0,728 09	0,729 92	0,731 66	0,733 32	0,734 88	0,736 33	0,737 69	0,738 94	0,740 09	0,741 12
480	0,726 27	0,727 77	0,729 27	0,730 70	0,732 04	0,733 30	0,734 47	0,735 55	0,736 54	0,737 43	0,738 23
500	0,726 25	0,727 49	0,728 72	0,729 88	0,730 97	0,731 97	0,732 90	0,733 74	0,734 51	0,735 19	0,735 79
520	0,726 24	0,727 25	0,728 25	0,729 18	0,730 04	0,730 84	0,731 56	0,732 21	0,732 79	0,733 29	0,733 72
540	0,726 23	0,727 04	0,727 84	0,728 58	0,729 25	0,729 87	0,730 41	0,730 89	0,731 31	0,731 67	0,731 96
560	0,726 22	0,726 87	0,727 49	0,728 06	0,728 57	0,729 03	0,729 43	0,729 77	0,730 05	0,730 27	0,730 44
580	0,726 21	0,726 71	0,727 19	0,727 61	0,727 99	0,728 31	0,728 57	0,728 79	0,728 96	0,729 07	0,729 13
600	0,726 21	0,726 58	0,726 92	0,727 22	0,727 47	0,727 68	0,727 84	0,727 95	0,728 01	0,728 03	0,728 00

Table B.4 — Coefficients for Equation (B.1) — Argon

i	a_i	b_i	c_i
1	$7{,}261\,844\,00 \times 10^{-1}$	0	0
2	$-1{,}173\,389\,76 \times 10^{-1}$	1	–4
3	$2{,}334\,785\,17 \times 10^{-1}$	1	–3
4	$-2{,}250\,904\,86 \times 10^{-3}$	1	0
5	$3{,}571\,311\,67 \times 10^{-2}$	1,5	–4
6	$9{,}236\,691\,04 \times 10^{-2}$	2	–9
7	$-7{,}882\,951\,14 \times 10^{-3}$	2	–3
8	$-4{,}050\,612\,00 \times 10^{-3}$	2	–2
9	$9{,}893\,033\,93 \times 10^{-5}$	2	0
10	$-1{,}502\,565\,89 \times 10^{-1}$	2,5	–8
11	$3{,}551\,149\,94 \times 10^{-1}$	3	–8
12	$1{,}400\,857\,98 \times 10^{-2}$	3	–4
13	$-1{,}511\,223\,06 \times 10^{-1}$	3,5	–8
14	$-2{,}569\,959\,78 \times 10^{-2}$	3,5	–5
15	$1{,}570\,106\,43 \times 10^{-2}$	4	–6

Critical parameters:

$p_c = 4{,}863$ MPa

$T_c = 150{,}687$ K

For argon, Equation (B.1) is valid over the temperature range 250 to 600 K at pressures up to 20 MPa. See [7] and [9].

Table B.5 gives values of C_* and Table B.6 coefficients for Equation (B.1) for dry air.

Table B.5 — C_* values — Dry air

T_0 K	p_0 MPa										
	0,1	**2**	**4**	**6**	**8**	**10**	**12**	**14**	**16**	**18**	**20**
200	0,685 90	0,705 14	0,728 11	0,754 14	0,782 77	0,812 51	0,841 06	0,866 13	0,886 30	0,901 24	0,911 32
220	0,685 66	0,699 86	0,715 94	0,733 15	0,751 19	0,769 46	0,787 13	0,803 37	0,817 52	0,829 20	0,838 33
240	0,685 48	0,696 22	0,707 95	0,720 05	0,732 36	0,744 59	0,756 36	0,767 32	0,777 16	0,785 65	0,792 71
260	0,685 34	0,693 60	0,702 38	0,711 22	0,720 02	0,728 63	0,736 88	0,744 57	0,751 55	0,757 70	0,762 96
280	0,685 21	0,691 64	0,698 34	0,704 95	0,711 43	0,717 69	0,723 64	0,729 18	0,734 23	0,738 72	0,742 61
300	0,685 09	0,690 13	0,695 29	0,700 32	0,705 17	0,709 81	0,714 19	0,718 25	0,721 94	0,725 24	0,728 10
320	0,684 97	0,688 93	0,692 94	0,696 79	0,700 46	0,703 93	0,707 18	0,710 18	0,712 89	0,715 31	0,717 40
340	0,684 85	0,687 96	0,691 08	0,694 03	0,696 81	0,699 42	0,701 84	0,704 04	0,706 03	0,707 78	0,709 29
360	0,684 71	0,687 15	0,689 57	0,691 83	0,693 93	0,695 87	0,697 66	0,699 27	0,700 70	0,701 94	0,702 99
380	0,684 55	0,686 46	0,688 31	0,690 02	0,691 59	0,693 03	0,694 32	0,695 46	0,696 46	0,697 31	0,698 00
400	0,684 38	0,685 85	0,687 25	0,688 52	0,689 67	0,690 70	0,691 60	0,692 38	0,693 04	0,693 57	0,693 98
420	0,684 19	0,685 29	0,686 33	0,687 25	0,688 06	0,688 76	0,689 35	0,689 84	0,690 23	0,690 51	0,690 69
440	0,683 97	0,684 78	0,685 52	0,686 15	0,686 68	0,687 12	0,687 46	0,687 72	0,687 89	0,687 97	0,687 96
460	0,683 74	0,684 30	0,684 79	0,685 18	0,685 49	0,685 71	0,685 85	0,685 91	0,685 90	0,685 82	0,685 66
480	0,683 49	0,683 84	0,684 12	0,684 32	0,684 43	0,684 48	0,684 45	0,684 36	0,684 21	0,683 99	0,683 70
500	0,683 22	0,683 39	0,683 50	0,683 53	0,683 49	0,683 39	0,683 23	0,683 01	0,682 73	0,682 40	0,682 02
520	0,682 93	0,682 96	0,682 92	0,682 81	0,682 65	0,682 42	0,682 15	0,681 82	0,681 44	0,681 02	0,680 55
540	0,682 62	0,682 53	0,682 37	0,682 15	0,681 87	0,681 54	0,681 17	0,680 76	0,680 30	0,679 80	0,679 26
560	0,682 30	0,682 10	0,681 84	0,681 52	0,681 15	0,680 74	0,680 29	0,679 80	0,679 27	0,678 71	0,678 11
580	0,681 97	0,681 68	0,681 33	0,680 93	0,680 49	0,680 00	0,679 48	0,678 93	0,678 35	0,677 73	0,677 09
600	0,681 63	0,681 27	0,680 84	0,680 37	0,679 86	0,679 32	0,678 74	0,678 14	0,677 51	0,676 85	0,676 16

Table B.6 — Coefficients for Equation (B.1) — Dry air

i	a_i	b_i	c_i
1	$1{,}967\ 947\ 91 \times 10^{-2}$	0	−3
2	$-2{,}774\ 414\ 35 \times 10^{-2}$	0	−1
3	$7{,}031\ 906\ 83 \times 10^{-1}$	0	0
4	$-3{,}448\ 411\ 43 \times 10^{-3}$	0	1
5	$-1{,}135\ 939\ 77 \times 10^{-1}$	1	−7
6	$1{,}507\ 325\ 95 \times 10^{-1}$	1	−3
7	$-2{,}403\ 454\ 97 \times 10^{-3}$	1	0
8	$1{,}224\ 631\ 76 \times 10^{-6}$	1	3
9	$-3{,}064\ 388\ 30 \times 10^{-3}$	2	−2
10	$2{,}116\ 285\ 54 \times 10^{-1}$	2,5	−8
11	$5{,}128\ 802\ 07 \times 10^{-5}$	2,5	0
12	$-1{,}666\ 687\ 29 \times 10^{-6}$	3	1
13	$-6{,}554\ 052\ 14 \times 10^{-2}$	3,5	−8
14	$1{,}390\ 831\ 40 \times 10^{-2}$	4	−8

Critical parameters:

p_c = 3,786 MPa

T_c = 132,530 6 K

For dry air, Equation (B.1) is valid over the temperature range 250 to 600 K at pressures up to 20 MPa. See [7] and [10].

Table B.7 gives values of C_* and Table B.8 coefficients for Equation (B.1) for methane.

Table B.7 — C_* values — Methane

T_0 K	p_0 MPa										
	0,1	**2**	**4**	**6**	**8**	**10**	**12**	**14**	**16**	**18**	**20**
200	—	—	—	—	—	—	—	—	—	—	—
220	0,674 04	0,707 10	0,757 33	0,840 96	0,992 20	1,163 38	—	—	—	—	—
240	0,673 23	0,697 96	0,731 18	0,775 54	0,835 85	0,912 11	0,989 36	1,049 30	1,088 02	1,109 75	1,119 53
260	0,672 29	0,691 35	0,715 15	0,743 81	0,778 22	0,818 18	0,861 09	0,902 06	0,936 53	0,962 60	0,980 60
280	0,671 19	0,686 19	0,704 03	0,724 26	0,747 03	0,772 03	0,798 39	0,824 59	0,848 87	0,869 83	0,88678
300	0,669 92	0,68189	0,695 66	0,710 68	0,726 91	0,744 13	0,761 92	0,779 64	0,796 56	0,812 00	0,825 46
320	0,668 50	0,678 15	0,688 98	0,700 49	0,712 59	0,725 13	0,737 88	0,750 51	0,762 68	0,774 03	0,784 30
340	0,666 96	0,674 80	0,683 44	0,692 43	0,701 72	0,711 18	0,720 67	0,730 02	0,739 04	0,747 54	0,755 36
360	0,665 32	0,671 73	0,678 69	0,685 82	0,693 08	0,700 39	0,707 64	0,714 75	0,721 59	0,728 06	0,734 06
380	0,663 63	0,668 89	0,674 54	0,680 25	0,686 00	0,691 73	0,697 37	0,702 87	0,708 15	0,713 14	0,717 79
400	0,661 93	0,666 26	0,670 85	0,675 46	0,680 05	0,684 59	0,689 03	0,693 33	0,697 45	0,701 34	0,704 97
420	0,660 25	0,663 81	0,667 56	0,671 29	0,674 97	0,678 59	0,682 11	0,685 50	0,688 73	0,691 78	0,694 63
440	0,658 60	0,661 53	0,664 59	0,667 61	0,670 58	0,673 47	0,676 27	0,678 95	0,681 49	0,683 89	0,686 11
460	0,657 00	0,659 40	0,661 90	0,664 35	0,666 73	0,669 05	0,671 27	0,673 39	0,675 39	0,677 27	0,679 00
480	0,655 47	0,657 43	0,659 46	0,661 44	0,663 35	0,665 19	0,666 95	0,668 62	0,670 18	0,671 64	0,672 98
500	0,654 01	0,655 61	0,657 24	0,658 82	0,660 35	0,661 80	0,663 18	0,664 49	0,665 70	0,666 82	0,667 84
520	0,652 62	0,653 91	0,655 21	0,656 47	0,657 67	0,658 81	0,659 88	0,660 88	0,661 80	0,662 64	0,663 39
540	0,651 31	0,652 33	0,653 36	0,654 34	0,655 27	0,656 14	0,656 96	0,657 70	0,658 39	0,659 00	0,659 53
560	0,650 07	0,650 87	0,651 66	0,652 41	0,653 11	0,653 76	0,654 36	0,654 90	0,655 38	0,655 80	0,656 15
580	0,648 91	0,649 51	0,650 10	0,650 66	0,651 16	0,651 63	0,652 04	0,652 40	0,652 71	0,652 97	0,653 18
600	0,647 80	0,648 24	0,648 66	0,649 05	0,649 39	0,649 70	0,649 96	0,650 17	0,650 34	0,650 46	0,650 54

Table B.8 — Coefficients for Equation (B.1) — Methane

i	a_i	b_i	c_i
1	$-4{,}720\,546\,92 \times 10^{-2}$	0	−1
2	$7{,}648\,102\,27 \times 10^{-1}$	0	0
3	$-5{,}034\,818\,10 \times 10^{-2}$	0	1
4	$5{,}707\,154\,95 \times 10^{-3}$	0	2
5	$-8{,}628\,216\,22 \times 10^{-2}$	0,5	−7
6	$2{,}310\,287\,94 \times 10^{-3}$	0,5	−4
7	$7{,}445\,647\,54 \times 10^{-1}$	1	−9
8	$-4{,}276\,642\,05 \times 10^{-1}$	1	−6
9	$3{,}289\,116\,00 \times 10^{-1}$	1	−4
10	$-2{,}068\,296\,47 \times 10^{-3}$	1	0
11	$-8{,}178\,634\,39 \times 10^{-1}$	1,5	−10
12	$1{,}868\,520\,89 \times 10^{-4}$	1,5	−1
13	$3{,}835\,357\,66 \times 10^{-1}$	2	−9
14	$-2{,}429\,634\,03 \times 10^{-3}$	3	−4
15	$2{,}802\,359\,69 \times 10^{-1}$	4	−15
16	$-1{,}226\,295\,45 \times 10^{-1}$	5	−15
17	$1{,}706\,268\,70 \times 10^{-4}$	5	−6
18	$1{,}582\,014\,74 \times 10^{-2}$	6	−14
19	$-3{,}733\,935\,09 \times 10^{-3}$	6	−12

Critical parameters:

$p_c = 4{,}592\,2$ MPa

$T_c = 190{,}564$ K

For methane, Equation (B.1) is valid over the temperature range 270 to 600 K at pressures up to 20 MPa. See [7] and [11].

Table B.9 gives values of C_* for carbon dioxide [12], Table B.10 those for oxygen [13] and Table B.11 those for steam.

Table B.9 — C_* values — Carbon dioxide

T_n K	p_n MPa										
	0,1	**2**	**4**	**6**	**8**	**10**	**12**	**14**	**16**	**18**	**20**
240	—	—	—	—	—	—	—	—	—	—	—
260	0,673 18	—	—	—	—	—	—	—	—	—	—
280	0,670 66	0,715 19	—	—	—	—	—	—	—	—	—
300	0,668 43	0,701 88	0,755 14	—	—	—	—	—	—	—	—
320	0,666 46	0,692 45	0,729 20	0,784 19	—	—	—	—	—	—	—
340	0,664 70	0,685 39	0,712 56	0,748 21	0,797 97	—	—	—	—	—	—
360	0,663 13	0,679 89	0,700 83	0,726 33	0,758 13	0,798 64	0,850 46	0,913 90	0,982 71	1,045 85	1,096 34
380	0,661 71	0,675 50	0,692 09	0,711 34	0,733 88	0,760 41	0,791 55	0,827 36	0,866 73	0,907 11	0,945 22
400	0,660 42	0,671 89	0,685 32	0,700 38	0,717 29	0,736 31	0,757 56	0,780 99	0,806 20	0,832 39	0,858 44
420	0,659 26	0,668 89	0,679 93	0,691 99	0,705 18	0,719 54	0,735 11	0,751 79	0,769 39	0,787 55	0,805 80
440	0,658 19	0,666 34	0,675 53	0,685 38	0,695 92	0,707 16	0,719 08	0,731 60	0,744 61	0,757 91	0,771 28
460	0,657 21	0,664 16	0,671 88	0,680 03	0,688 62	0,697 63	0,707 03	0,716 77	0,726 77	0,736 92	0,747 08
480	0,656 31	0,662 26	0,668 80	0,675 62	0,682 72	0,690 07	0,697 65	0,705 42	0,713 32	0,721 28	0,729 22
500	0,655 48	0,660 60	0,666 18	0,671 93	0,677 86	0,683 94	0,690 15	0,696 45	0,702 82	0,709 20	0,715 54
520	0,654 71	0,659 13	0,663 91	0,668 80	0,673 79	0,678 87	0,684 02	0,689 21	0,694 42	0,699 61	0,704 75
540	0,653 99	0,657 82	0,661 93	0,666 11	0,670 34	0,674 62	0,678 92	0,683 24	0,687 55	0,691 83	0,696 05
560	0,653 32	0,656 65	0,660 19	0,663 77	0,667 38	0,671 00	0,674 63	0,678 25	0,681 85	0,685 40	0,688 90
580	0,652 69	0,655 58	0,658 65	0,661 73	0,664 82	0,667 90	0,670 97	0,674 02	0,677 04	0,680 01	0,682 93
600	0,652 10	0,654 62	0,657 28	0,659 93	0,662 58	0,665 21	0,667 82	0,670 40	0,672 95	0,675 45	0,677 89

Table B.10 — C_* values — Oxygen

T_0 K	p_0 MPa											
	0	**0,5**	**1**	**2**	**3**	**4**	**5**	**6**	**7**	**8**	**9**	**10**
223,15	0,684 6	0,688 6	0,692 7	0,701 3	0,710 4	0,720 1	0,730 4	0,741 3	0,752 8	0,765 0	0,777 9	0,791 4
248,15	0,684 5	0,687 5	0,690 5	0,696 6	0,703 0	0,709 6	0,716 4	0,723 4	0,730 7	0,738 1	0,745 7	0,753 5
273,15	0,684 4	0,686 6	0,688 9	0,693 4	0,698 1	0,702 8	0,707 6	0,712 5	0,717 5	0,722 5	0,727 6	0,732 6
298,15	0,684 2	0,685 9	0,687 6	0,691 1	0,694 6	0,698 1	0,701 6	0,705 2	0,708 7	0,712 3	0,715 9	0,719 4
323,15	0,683 9	0,685 2	0,686 5	0,689 2	0,691 9	0,694 5	0,697 2	0,699 9	0,702 5	0,705 1	0,707 8	0,710 3
348,15	0,683 5	0,684 5	0,685 5	0,687 6	0,689 7	0,691 7	0,693 8	0,695 8	0,697 8	0,699 8	0,701 7	0,703 7
373,15	0,682 9	0,683 7	0,684 5	0,686 1	0,687 7	0,689 3	0,690 9	0,692 5	0,694 0	0,695 5	0,697 0	0,698 4

Table B.11 — C_* values — Steam (single-phase gas)

T_0 K	p_0 MPa										
	0,1	**2**	**4**	**6**	**8**	**10**	**12**	**14**	**16**	**18**	**20**
420	0,673 38	—	—	—	—	—	—	—	—	—	—
440	0,672 72	—	—	—	—	—	—	—	—	—	—
460	0,672 09	—	—	—	—	—	—	—	—	—	—
480	0,671 49	—	—	—	—	—	—	—	—	—	—
500	0,670 91	—	—	—	—	—	—	—	—	—	—
520	0,670 35	—	—	—	—	—	—	—	—	—	—
540	0,669 82	0,689 77	—	—	—	—	—	—	—	—	—
560	0,669 30	0,686 41	—	—	—	—	—	—	—	—	—
580	0,668 79	0,683 58	0,702 47	—	—	—	—	—	—	—	—
600	0,668 30	0,681 19	0,697 15	0,716 39	—	—	—	—	—	—	—
620	0,667 81	0,679 13	0,692 78	0,708 75	0,727 78	0,751 02	—	—	—	—	—
640	0,667 34	0,677 32	0,689 14	0,702 60	0,718 17	0,736 49	0,758 52	—	—	—	—
660	0,666 87	0,675 73	0,686 04	0,697 57	0,710 57	0,725 41	0,742 60	0,762 88	0,787 38	—	—
680	0,666 42	0,674 31	0,683 38	0,693 35	0,704 40	0,716 73	0,730 61	0,746 42	0,764 67	0,786 09	0,811 77
700	0,665 97	0,673 02	0,681 05	0,689 77	0,699 28	0,709 72	0,721 23	0,734 02	0,748 34	0,764 53	0,783 02
720	0,665 52	0,671 86	0,679 00	0,686 67	0,694 95	0,703 92	0,713 65	0,724 28	0,735 92	0,748 77	0,763 01
740	0,665 08	0,670 79	0,677 17	0,683 97	0,691 24	0,699 02	0,707 38	0,716 37	0,726 09	0,736 61	0,748 04
760	0,664 65	0,669 80	0,675 53	0,681 59	0,688 01	0,694 84	0,702 09	0,709 81	0,718 06	0,726 88	0,736 33
780	0,664 22	0,668 89	0,674 05	0,679 47	0,685 18	0,691 21	0,697 56	0,704 27	0,711 37	0,718 89	0,726 86
800	0,663 80	0,668 04	0,672 70	0,677 57	0,682 68	0,688 03	0,693 64	0,699 52	0,705 70	0,712 19	0,719 02
820	0,663 38	0,667 24	0,671 46	0,675 86	0,680 44	0,685 22	0,690 20	0,695 40	0,700 83	0,706 49	0,712 41
840	0,662 96	0,666 48	0,670 32	0,674 30	0,678 43	0,682 72	0,687 17	0,691 79	0,696 59	0,701 57	0,706 75
860	0,662 55	0,665 77	0,669 27	0,672 88	0,676 61	0,680 48	0,684 47	0,688 60	0,692 87	0,697 29	0,701 85
880	0,662 15	0,665 09	0,668 28	0,671 57	0,674 96	0,678 45	0,682 05	0,685 76	0,689 58	0,693 51	0,697 57
900	0,661 75	0,664 45	0,667 37	0,670 37	0,673 45	0,676 61	0,679 87	0,683 21	0,686 64	0,690 17	0,693 79
920	0,661 35	0,663 83	0,666 51	0,669 25	0,672 06	0,674 94	0,677 89	0,680 91	0,684 01	0,687 18	0,690 43
940	0,660 96	0,663 24	0,665 69	0,668 21	0,670 77	0,673 40	0,676 08	0,678 83	0,681 63	0,684 50	0,687 42
960	0,660 57	0,662 67	0,664 93	0,667 23	0,669 58	0,671 98	0,674 43	0,676 93	0,679 47	0,682 07	0,684 72
980	0,660 19	0,662 13	0,664 20	0,666 32	0,668 48	0,670 67	0,672 91	0,675 19	0,677 51	0,679 87	0,682 27
1 000	0,659 81	0,661 60	0,663 51	0,665 46	0,667 44	0,669 46	0,671 51	0,673 59	0,675 71	0,677 86	0,680 04

Annex C
(normative)

Computation of critical mass flux for natural gas mixtures

C.1 General

This annex provides the necessary information for calculating the critical mass flux of natural gas mixtures. The correlation calculates the mass flux, $q_m/A_{nt}C_{d'}$, directly and is expressed in terms of temperature, pressure and gas composition.

The correlation is divided into three composition ranges by the mole fraction content of ethane in the gas mixture in question:

Range 1 0,01 to 0,045

Range 2 0,045 to 0,08

Range 3 0,08 to 0,115

The recommended mole fraction limits for which the correlation is applicable are given in Table C.1.

Table C.1 — Recommended mole fraction limits

Component	Range 1	Range 2	Range 3
Methane	0,89–0,98	0,84–0,93	0,79–0,88
Ethane	0,01–0,045	0,045–0,08	0,08–0,115
Propane	0,002–0,02	0,008–0,03	0,015–0,04
Butane	0,0–0,005	0,002–0,01	0,003–0,015
Pentane	0,0–0,002	0,0–0,004	0,0–0,005
Hexane +	0,0–0,001 5	0,0–0,002	0,0–0,003
Nitrogen	0,0–0,03	0,0–0,03	0,0–0,015
Carbon dioxide	0,0–0,025	0,0–0,025	0,01–0,025

The correlation is valid in the temperature range 270 to 320 K at pressures up to 12 MPa. Note that mole fractions should add to unity.

If a natural gas mixture does not fit with the fraction limit of one composition range given above, it is recommended that the composition range for which the mole fraction content of ethane is the closest be used. In such cases, the relative uncertainty on $q_m/A_{nt}C_{d'}$ is increased from 0,10 % to 0,15 % at 95 % confidence.

C.2 Correlation

$$\frac{q_m}{A_{nt}C_{d'}} = q_{ref} + S \times f \qquad \text{(C.1)}$$

where

q_{ref} is the mass flux of a reference gas;

S is the sensitivity of the mass flux to a change in composition;

f is a composition dependent factor.

The general form for each of these terms is given in Equations (C.2) to (C.4):

$$q_{\text{ref}} = \sum_i a_i \pi^{\alpha_i} \tau^{\phi_i} \tag{C.2}$$

$$S = \sum_i b_i \pi^{\gamma_i} \tau^{\delta_i} \tag{C.3}$$

$$f = X_{\text{C}_2} + \sum_{i=\text{C}_3}^{\text{C}_6} A_i X_i + \left[A_{\text{N}_2} - \left(B_{\text{N}_2} - C_{\text{N}_2} \tau \right) \pi \right] X_{\text{N}_2} + \left[A_{\text{CO}_2} - \left(B_{\text{CO}_2} - C_{\text{CO}_2} \tau \right) \pi \right] X_{\text{CO}_2} - A_{\text{ref}} \tag{C.4}$$

$$\pi = \frac{p_0}{p_{\text{ref}}} \text{ and } \tau = \frac{T_0}{T_{\text{ref}}}$$

where $p_{\text{ref}} = 5$ MPa and $T_{\text{ref}} = 200$ K.

The coefficients for q_{ref} and S for the three composition ranges are given in Tables C.2, C.3 and C.4. The coefficients for f for the three composition ranges are given in Table C.5.

See [14].

C.3 Nozzle throat to pipe diameter ratio, β

The values provided in this annex apply to cases where $\beta < 0{,}25$. If this condition is not met, there will be a small but significant velocity at the upstream measurement point. In such circumstances, the user should also apply the mass flow correction factor given in Annex E.

Table C.2 — Coefficients of q_{ref} and S for Equations (C.2) and (C.3) — First composition range

k	a	α	ϕ	b	γ	δ
1	$0{,}108\,244\,635 \times 10^{5}$	1	−0,5	$0{,}484\,093\,947 \times 10^{4}$	1	−4,5
2	$-0{,}736\,494\,058 \times 10^{2}$	1	1,5	$-0{,}136\,051\,287 \times 10^{5}$	1	−2,5
3	$-0{,}287\,636\,821 \times 10^{4}$	2	−9,5	$0{,}132\,819\,568 \times 10^{5}$	1	−1,5
4	$0{,}293\,505\,438 \times 10^{4}$	2	−4,5	$0{,}124\,742\,840 \times 10^{3}$	1,5	−0,5
5	$0{,}213\,321\,640 \times 10^{3}$	2,5	−3,5	$0{,}270\,400\,184 \times 10^{4}$	2	−4,5
6	$0{,}470\,680\,038 \times 10^{4}$	3,5	−12,5	$0{,}465\,931\,801 \times 10^{4}$	2,5	−5,5
7	$-0{,}113\,603\,383 \times 10^{1}$	5	−0,5	$-0{,}522\,305\,671 \times 10^{5}$	3,5	−15,5
8	$-0{,}949\,791\,998 \times 10^{1}$	9	−15,5	$0{,}728\,305\,715 \times 10^{5}$	4	−15,5
9	—	—	—	$0{,}626\,536\,557 \times 10^{1}$	4	−0,5
10	—	—	—	$0{,}863\,837\,290 \times 10^{1}$	6	−8,5
11	—	—	—	$-0{,}218\,148\,488 \times 10^{1}$	6	−0,5
12	—	—	—	$-0{,}205\,507\,321 \times 10^{3}$	9	−15,5
13	—	—	—	$0{,}172\,829\,796 \times 10^{1}$	11	−10,5
14	—	—	—	$0{,}366\,195\,951 \times 10^{-2}$	16	−10,5

Table C.3 — Coefficients of q_{ref} and S for Equations (C.2) and (C.3) — Second composition range

k	a	α	ϕ	b	γ	δ
1	$0{,}110\,966\,325 \times 10^{5}$	1	−0,5	$0{,}598\,807\,893 \times 10^{0}$	0	−0,5
2	$-0{,}812\,543\,416 \times 10^{2}$	1	1,5	$0{,}618\,961\,744 \times 10^{3}$	1	−1,5
3	$-0{,}297\,016\,307 \times 10^{4}$	2	−6,5	$0{,}302\,809\,257 \times 10^{4}$	1	−0,5
4	$0{,}433\,774\,605 \times 10^{4}$	2	−4,5	$0{,}134\,089\,681 \times 10^{4}$	1,5	−3,5
5	$0{,}148\,426\,025 \times 10^{4}$	3	−7,5	$0{,}523\,229\,697 \times 10^{3}$	2	−1,5
6	$0{,}704\,694\,512 \times 10^{4}$	4	−15,5	$-0{,}862\,689\,783 \times 10^{4}$	3	−8,5
7	$-0{,}254\,996\,358 \times 10^{1}$	4,5	−0,5	$0{,}235\,424\,200 \times 10^{5}$	3	−7,5
8	$-0{,}224\,612\,799 \times 10^{2}$	9	−15,5	$-0{,}767\,928\,108 \times 10^{3}$	3,5	−3,5
9	—	—	—	$-0{,}859\,071\,767 \times 10^{5}$	4,5	−12,5
10	—	—	—	$0{,}724\,778\,127 \times 10^{4}$	4,5	−8,5
11	—	—	—	$0{,}153\,097\,473 \times 10^{6}$	5	−15,5
12	—	—	—	$-0{,}135\,420\,339 \times 10^{4}$	6	−10,5
13	—	—	—	$-0{,}292\,807\,154 \times 10^{5}$	7	−20,5
14	—	—	—	$0{,}884\,153\,806 \times 10^{-1}$	16	−15,5

Table C.4 — Coefficients of q_{ref} and S for Equations (C.2) and (C.3) — Third composition range

k	a	α	ϕ	b	γ	δ
1	$0{,}115\,572\,303 \times 10^{5}$	1	−0,5	$0{,}801\,874\,088 \times 10^{3}$	1	−1,5
2	$-0{,}249\,894\,765 \times 10^{3}$	1	0,5	$0{,}264\,127\,915 \times 10^{4}$	1	−0,5
3	$-0{,}240\,531\,018 \times 10^{4}$	2	−7,5	$0{,}247\,996\,282 \times 10^{3}$	1,25	−0,5
4	$0{,}404\,006\,226 \times 10^{4}$	2	−4,5	$0{,}178\,851\,521 \times 10^{4}$	2	−8,5
5	$0{,}271\,706\,092 \times 10^{4}$	3	−7,5	$0{,}101\,397\,979 \times 10^{5}$	2,5	−5,5
6	$-0{,}126\,049\,305 \times 10^{5}$	4	−15,5	$-0{,}296\,058\,326 \times 10^{2}$	3,5	−0,5
7	$0{,}553\,331\,233 \times 10^{5}$	5	−18,5	$-0{,}680\,911\,912 \times 10^{5}$	4	−15,5
8	$-0{,}115\,934\,413 \times 10^{3}$	5	−7,5	$0{,}259\,571\,626 \times 10^{6}$	5	−18,5
9	$-0{,}262\,586\,997 \times 10^{5}$	6	−20,5	$-0{,}144\,795\,597 \times 10^{6}$	7	−25,5
10	—	—	—	$-0{,}110\,728\,705 \times 10^{4}$	9	−15,5
11	—	—	—	$0{,}144\,085\,124 \times 10^{2}$	11	−10,5
12	—	—	—	$0{,}901\,740\,847 \times 10^{0}$	16	−15,5
13	—	—	—	$-0{,}132\,368\,505 \times 10^{0}$	16	−10,5

Table C.5 — Coefficients for f for Equation (C.4)

Coefficient	Range 1	Range 2	Range 3
A_{C_3}	2,011 3	2,157 5	2,244 0
A_{C_4}	2,751 7	2,803 4	3,123 8
A_{C_5}	3,889 8	4,086 0	4,316 1
A_{C_6}	4,947 8	5,423 0	5,869 3
A_{N_2}	1,014 8	1,041 1	1,107 4
B_{N_2}	1,464 3	1,672 1	2,268 9
C_{N_2}	0,765 0	0,879 4	1,222 4
A_{CO_2}	2,253 3	2,348 8	2,434 7
B_{CO_2}	1,673 3	2,002 4	2,125 0
C_{CO_2}	0,881 9	1,065 9	1,125 1
A_{ref}	0,066 36	0,136 94	0,217 73

C.4 Sample values for computer code verification

Tables C.6 and C.7 present sample values against which the user can verify the implementation of the correlation.

Table C.6 — Sample values for verifying implementation of correlation

Component	Test gas 1	Test gas 2	Test gas 3
Methane	0,931 7	0,880 5	0,837 5
Nitrogen	0,024 3	0,010 4	0,003 9
Carbon dioxide	0,009 5	0,020 4	0,019 7
Ethane	0,026 3	0,062 4	0,093 5
Propane	0,004 9	0,018 4	0,033 1
Butane	0,002 0	0,006 1	0,009 7
Pentane	0,001 3	0,001 5	0,002 0
Hexane	0,000 0	0,000 3	0,000 6

Table C.7 — Sample values for verifying implementation of correlation

	T_0 K	p_0 MPa	q_{ref}	S	f	$q_m/(A_{nt}C_{d'})$
Test gas 1	280	2	3 704,50	1 481,33	0,020 94	3 735,52
	310	10	19 007,4	10 716,5	0,007 07	19 083,2
Test gas 2	280	2	3 805,42	1 402,57	0,042 76	3 865,38
	310	10	19 749,8	10 905,8	0,028 04	20 055,5
Test gas 3	280	2	3 913,25	1 325,58	0,039 58	3 965,72
	310	10	20 603,1	11 260,7	0,026 85	20 905,5

Annex D
(normative)

Mass flow correction factor for atmospheric air

D.1 General

The mass flow of atmospheric air, $q_{m,atmos}$, for a given upstream stagnation temperature, T_0 (K), and pressure, p_0 (MPa), can be calculated from Equation (D.1):

$$q_{m,\text{atmos}} = q_{m,\text{dryCO}_2\text{-free}} \left[1 + X_{CO_2} \left(0{,}25 + 0{,}047\,32\pi \right) + \frac{RH}{100} A \cdot B \right] \quad \text{(D.1)}$$

where

$q_{m,\text{dryCO}_2\text{-free}}$ is the mass flow of dry CO_2-free air;

X_{CO_2} is the mole fraction of CO_2 in the air (if not known, use 0,000 4);

RH is the relative humidity (%) of the air;

$$A = 0{,}127\,828\,\tau^3 - 0{,}789\,422\,\tau^2 + 1{,}631\,66\,\tau - 1{,}128\,18 \quad \text{(D.2)}$$

where

$$\tau = \frac{T_0}{T_c}$$

$$B = -0{,}000\,288\,749\,\pi^2 - 0{,}001\,910\,22\,\pi + 0{,}005\,695\,36 - \frac{0{,}071\,999\,5}{\pi} \quad \text{(D.3)}$$

where

$$\pi = \frac{p_0}{p_c}$$

where $p_c = 3{,}786$ MPa and $T_c = 132{,}530\,6$ K.

D.2 Sample values for computer code verification

Table D.1 shows sample values against which the user can verify their implementation of the correlation.

Table D.1 — Sample values for verifying implementation of correlation

T K	p MPa	RH %	$q_{m,\text{dryCO}_2\text{-free}}$	$q_{m,\text{atmos}}$
280	0,1	50	241,663	241,403
280	1	100	2 427,42	2 427,11
305	0,1	75	231,501	229,674
305	2	100	4 662,04	4 660,15

Annex E
(normative)

Computation of critical mass flux for critical flow nozzles with high nozzle throat to upstream pipe diameter ratio, $\beta > 0{,}25$

E.1 General

The values obtained for the mass flow of a gas using the methods given in Annex B or C are based on the assumption that the measured upstream temperature and pressure are the true stagnation values. This assumption will be valid if the nozzle throat to upstream pipe diameter ratio, $\beta < 0{,}25$. If this is in fact the case, there will be a significant gas velocity at the upstream measurement point, which will significantly affect the mass flow-rate.

When there is a significant gas velocity at the upstream measurement point, the pressure tapping will measure the static pressure, i.e. the pressure of the moving gas. However, the temperature is measured using a thermometer inserted into the flowing gas. This causes the gas to slow down as it encounters the probe, causing the probe to record a temperature, T_{m}, that is neither the stagnation temperature, T_0, nor the static temperature, T_{s}, but somewhere in between. The relationship between the temperatures is given by the temperature probe recovery factor:

$$R_{\mathrm{f}} = \frac{T_{\mathrm{m}} - T_{\mathrm{s}}}{T_0 - T_{\mathrm{s}}} \tag{E.1}$$

For R_{f}, a value of zero means that the probe is measuring the static temperature, T_{s}, whilst a value of 1 means it is the stagnation temperature, T_0, being measured. In practice, R_{f} is generally in the range 0,5 to 0,9, implying that the measured temperature is closer to the stagnation temperature than the static temperature.

E.2 Correction factors

IMPORTANT — At the time of publication of this International Standard, correction factors for natural gas mixtures had not been established. If a correction factor for a natural gas mixture is required, then that for methane should be used.

The following correction factor is applicable to the same gases as Equation (B.1): namely, nitrogen, argon, dry CO_2-free air and methane. The valid temperature and pressure range is also the same, 250 K – 600 K (270 K – 600 K for methane) and up to 20 MPa. The correction is valid for β values from 0,25 to 0,5.

The mass flow through a nozzle with a high β (0,15 to 0,5), $q_{m,\beta}$, for a given upstream measured temperature, T_{m} (K), and pressure p_{m} (MPa), can be calculated from:

$$q_{m,\beta} = q_{m,\mathrm{stag}} \left[\left(1 - R_{\mathrm{f}}\right) F_0 + R_{\mathrm{f}} F_1 \right] \tag{E.2}$$

where

$q_{m,\mathrm{stag}}$ is the mass flow-rate as calculated using Annex B or C;

R_{f} is the temperature probe recovery factor.

The correction factors, F_0 and F_1 take the form:

$$F_i = 1 + B \cdot C_i \tag{E.3}$$

where

$$B = 25{,}879\ \beta^6 - 32{,}693\ \beta^5 + 34{,}276\ \beta^4 - 6{,}019\ 9\ \beta^3 + 1{,}115\ 6\ \beta^2 - 0{,}112\ 2\ \beta + 0{,}004\ 7 \quad \text{(E.4)}$$

and

$$C_i = \sum_k n_{i,k} \pi^{p_{i,k}} \tau^{t_{i,k}} \quad \text{(E.5)}$$

The coefficients for Equation (E.5) are given in Tables E.1 to E.4. For the critical parameters required to obtain the reduced pressure and temperature, π and τ, see Annex B.

See [15].

Table E.1 — Coefficients for Equation (E.5) for nitrogen

i	k	$n_{i,k}$	$p_{i,k}$	$t_{i,k}$
0	1	$1{,}304\ 619 \times 10^{-2}$	0	0
	2	$-3{,}666\ 323 \times 10^{-5}$	0	1
	3	$-3{,}668\ 820 \times 10^{-3}$	0,5	−5
	4	$5{,}024\ 075 \times 10^{-4}$	1	−1
	5	$2{,}846\ 962 \times 10^{-3}$	2	−6
	6	$-7{,}569\ 285 \times 10^{-4}$	3	−8
1	1	$1{,}516\ 890 \times 10^{-2}$	0	0
	2	$-2{,}433\ 804 \times 10^{-5}$	0	1
	3	$-3{,}755\ 322 \times 10^{-3}$	1	−3
	4	$4{,}068\ 331 \times 10^{-3}$	1	−2
	5	$9{,}540\ 179 \times 10^{-3}$	1,5	−6
	6	$-4{,}828\ 687 \times 10^{-6}$	5	−6

Table E.2 — Coefficients for Equation (E.5) for argon

i	k	$n_{i,k}$	$p_{i,k}$	$t_{i,k}$
0	1	$1{,}359\ 113 \times 10^{-2}$	0	0
	2	$5{,}072\ 601 \times 10^{-4}$	1	−1
	3	$5{,}776\ 326 \times 10^{-4}$	2	−4
	4	$4{,}625\ 040 \times 10^{-4}$	3	−10
	5	$-3{,}001\ 709 \times 10^{-7}$	6	−4
1	1	$1{,}702\ 515 \times 10^{-2}$	0	0
	2	$3{,}255\ 007 \times 10^{-3}$	1	−2
	3	$2{,}029\ 543 \times 10^{-4}$	1	−1
	4	$6{,}931\ 127 \times 10^{-3}$	2	−6
	5	$-1{,}846\ 055 \times 10^{-4}$	4	−6

Table E.3 — Coefficients for Equation (E.5) for dry CO_2-free air

i	k	$n_{i,k}$	$p_{i,k}$	$t_{i,k}$
0	1	$1{,}307\,864 \times 10^{-2}$	0	0
	2	$-4{,}752\,544 \times 10^{-5}$	0	1
	3	$1{,}760\,268 \times 10^{-2}$	0,5	−6
	4	$-1{,}340\,098 \times 10^{-2}$	0,5	−5
	5	$4{,}672\,622 \times 10^{-4}$	1	−1
	6	$1{,}294\,203 \times 10^{-3}$	1,5	−4
1	1	$1{,}522\,775 \times 10^{-2}$	0	0
	2	$-4{,}726\,879 \times 10^{-5}$	0	1
	3	$-5{,}958\,875 \times 10^{-3}$	1	−4
	4	$3{,}445\,387 \times 10^{-3}$	1	−2
	5	$1{,}256\,916 \times 10^{-2}$	1,5	−6
	6	$-4{,}775\,091 \times 10^{-5}$	4	−6

Table E.4 — Coefficients for Equation (E.5) for methane

i	k	$n_{i,k}$	$p_{i,k}$	$t_{i,k}$
0	1	$1{,}068\,826 \times 10^{-3}$	0	−1
	2	$1{,}199\,593 \times 10^{-2}$	0	0
	3	$-1{,}482\,920 \times 10^{-3}$	0,5	−6
	4	$2{,}764\,799 \times 10^{-4}$	1	−1
	5	$7{,}920\,711 \times 10^{-5}$	2	−2
	6	$1{,}111\,278 \times 10^{-3}$	3	−8
	7	$-6{,}815\,626 \times 10^{-5}$	5	−10
	8	$3{,}862\,490 \times 10^{-8}$	10	−18
1	1	$-3{,}463\,148 \times 10^{-3}$	0	−3
	2	$5{,}286\,029 \times 10^{-3}$	0	−1
	3	$1{,}195\,016 \times 10^{-2}$	0	0
	4	$1{,}664\,232 \times 10^{-3}$	1	−2
	5	$1{,}159\,371 \times 10^{-3}$	1,5	−4
	6	$7{,}260\,461 \times 10^{-3}$	3	−10
	7	$-7{,}541\,933 \times 10^{-4}$	5	−12
	8	$2{,}613\,967 \times 10^{-7}$	10	−15

Bibliography

[1] ISO 5167-1:2003, *Measurement of fluid flow by means of pressure differential devices inserted in circular cross-section conduits running full — Part 1: General principles and requirements*

[2] ISO 5167-2:2003, *Measurement of fluid flow by means of pressure differential devices inserted in circular cross-section conduits running full — Part 2: Orifice plates*

[3] ISO 6976:1995, *Natural gas — Calculation of calorific values, density, relative density and Wobbe index from composition*

[4] STARLING, K.E., SAVIDGE, J.L. *Compressibility factors for natural gas and related hydrocarbon gases*. Second edition, Transmission Measurement Committee Report No. 8. AGA November 1992, also Errata N° 1 issued by AGA June 1993

[5] CARON, R.W., BRITTON, C.L., KEGEL, T. *Investigation into the premature unchoking phenomena of critical flow venturis*, Proceedings of ASME FEDSM2000-11108, Boston, June 2000

[6] ISO 5168, *Measurement of fluid flow — Procedure for the evaluation of uncertainties*

[7] STEWART, D.G., WATSON, J.T.R. and VAIDYA, A.M. Improved critical flow factors and representative equations for four calibration gases. *Flow Measurement and Instrumentation*, 1999, 10 (1): 27-34

[8] SPAN, R., LEMMON, E.W., JACOBSEN, R.T., and WAGNER, W. A Reference Quality Equation of State for Nitrogen. *International Journal of Thermophysics*, 1998; 19(4): 1121-1132

[9] TEGELER, CH., SPAN, R., and WAGNER, W. A new equation of state for argon covering the fluid region from the triple-point temperature to 700 K at pressures up to 1000 MPa. Paper Presented at *13th Symposium on Thermophysical Properties*, Boulder, June 1997

[10] PANASATI, M.D., LEMMON, E.W., PENONCELLO, S.G., JACOBSEN, R.T., and FRIEND, D.G. Thermodynamic properties of air from 60 to 2000 K at pressures up to 2000 MPa. Paper Presented at *13th Symposium on Thermophysical Properties*, Boulder, June 1997

[11] SETZMANN, U. and WAGNER, W. A new equation of state and tables of thermodynamic properties for methane covering the range from the melting line to 625 K at pressures up to 1 000 MPa. *Journal of Physical and Chemical Reference Data*, 1991; 20(6): 1061-1116.

[12] SPAN, R. and WAGNER, W. A New Equation of State for Carbon Dioxide Covering the Fluid Region from the Triple-Point Temperature to 1100 K at Pressures up to 800 MPa. *Journal of Physical and Chemical Reference Data*, 1996; 25(6): 1509-1596

[13] MILLER, R.W. *Flow measurement engineering handbook*. McGraw-Hill, 1983

[14] STEWART, D.G., WATSON, J.T.R., and VAIDYA, A.M. A new correlation for the critical mass flux of natural mixtures. *Flow Measurement and Instrumentation*, 11 (4), December 2000

[15] STEWART, D.G., WATSON, J.T.R., and VAIDYA, A.M. The effect of high beta values on mass flow through critical flow nozzles. *Flow Measurement and Instrumentation*, Volume 11 Number 4, December 2000

[16] JAESCHKE, M., AUDIBERT, S., VAN CANEGHEM, P., HUMPHREYS, A.E., JANSSEN-VAN ROSMALEN, R., PELLEI, Q., MHICHELS, J.P.J., SCHOUTEN, J.A., TEN SELDAM, C.A. High accuracy compressibility factor calculation for natural gases and similar mixtures by use of a truncated virial equation, *GERG Technical Monograph TM2* (1988), and *Fortschritt-Berichte VDI, Series 6, N°231* (1989)

[17] STEWART, D.G., WATSON, J.T.R. and VAIDYA, A.M. Uncertainty in the theoretical mass flow-rate of pure gases through critical flow nozzles. *Int. Fluid Flow Measurement Symposium*, Denver, 27-30 June 1999

[18] STEWART, D.G., WATSON, J.T.R., VAIDYA, A.M. The effect of using atmospheric air in Critical Flow Nozzles. Int. Fluid Flow Measurement Symposium, Denver, 27-30 June 1999

[19] KEGEL, T. A study of the repeatabiliy and reproducibility of the Critical Flow Nozzle. *Int. Fluid Flow Measurement Symposium*, Denver 27-30 June, 1999

[20] CARON, R.W., BRITTON, C.L., KEGEL, T. Investigation into the accuracy of multiple Critical Flow Venturis mounted in parallel within a common plenum. *Int. Fluid Flow Measurement Symposium*, Denver 27-30 June, 1999

[21] PARK, K.A., CHOI, Y.M., CHOI, H.M., CHA, T.S., YOON, B.H. The evaluation of critical pressure ratios of sonic nozzle at low Reynolds numbers, released for *Flow. Meas. Instrum.*

[22] STUDZINSKI, W., WILLIAMSON, I.D., JUNGOWSKI, W., BOTROS, K.K., SAWCHUK, B., STROM, V. Nova's gravimetric meter prover and sonic nozzle facility, *CGA Gas Measurement School*, Alberta, Canada, 1994

[23] CHOI, Y.M., PARK, K.A., PARK S.O. Interference effects between sonic nozzles, *Flow. Meas. Instrum. 8*, page 113-119, 1997

[24] CHOI, Y.M., PARK, K.A., PARK, J.T., CHOI, H.M., PARK S.O. Interference effects of three sonic nozzles of different throat diameters in the same meter tube, *Flow. Meas. Instrum. 10*, page 175-181, 1999

[25] ISHIBASHI, M., TAKAMOTO, M. Theorical discharge coefficient of a critical circular-arc nozzle with laminar boundary layer and its verification by measurements using super-accurate nozzles, Flow Measurement and Instrumentation 11, 305/313, 2000

[26] VON LAVANTE, E., NATH, B., DIETRICH, H. Effects of instabilities on flow-rates in small sonic nozzles, *9th Conference on Flow Measurement FLOMEKO'98*, Lund, 1998

Discharge coefficients for toroidal-throat Venturi nozzles

[27] BRAIN, T.J.S. and MACDONALD, L.M. Evaluation of the performance of small-scale critical flow venturi using the NEL gravimetric gas flow standard test facility. *Fluid Flow Measurement in the Mid 1970s*. Edinburgh: HMSO, 1977, pp. 103-125

[28] BRAIN, T.J.S. and REID, J. Primary calibration of critical flow venturis in high-pressure gas. *Flow Measurement of Fluids,* edited by DIJSTELBERGEN, H.H. and SPENCER, E.A. Amsterdam: North Holland Publishing, 1978, pp 54-64

[29] SMITH, R.E. and MATZ, R.J. A theoretical method of determining discharge coefficients for Venturis operating at critical flow conditions. *J. Bas. Engng.,* 1962, vol. 84, No. 4, pp. 434-446

[30] ARNBERG, B.T., BRITTON, C.L. and SEIDL, W.F. Discharge coefficient correlations for circular arc venturi flowmeters at critical (sonic) flow. *Paper No. 73-WA/FM-8.* New York: American Society of Mechanical Engineers, 1973

[31] BRAIN, T.J.S. and REID, J. An investigation of the discharge coefficient characteristics and manufacturing specification of toroidal inlet critical flow venturi nozzles proposed as standard ISO flowmeters. *Proceedings of the International Conference on Advances in Flow Measurement, Paper C1,* University of Warwick. Cranfield, Bedford: BHRA Fluid Engineering, 1981

[32] SPENCER, E.A., EUJEN, E., DIJSTELBERGEN, H.H. and PEIGNELIN, G. Intercomparison campaign on high pressure gas flow test facilities. *EEC Document No. EUfR 6662.* Brussels-Luxembourg: ECSC-EEC-EAEC, 1980

[33] KARNIK, U., BOWLES, E.B., BOSIO, J., CALDWELL, S. North American Inter-Laboratory Flow Measurement Testing Program. *North Sea Flow Measurement Workshop 1996* — Peebles, Scotland. Paper No. 3

[34] ISHIBASHI, M., TAKAMOTO, M. Very Accurate Analytical Calculation of the Discharge Coefficients of Critical Venturi Nozzles with Laminar Boundary Layer. *FLUCOME'97*, Hayama

[35] ISHIBASHI, M., TAKAMOTO, M. Discharge coefficient of superaccurate critical nozzle at pressurised condition. *Int. Fluid Flow Measurement Symposium*, Denver 27-30 June, 1999

[36] ARNBERG, B.T. and ISHIBASHI, M. Discharge coefficient equations for critical flow Toroidal-throat Venturi nozzles, *Proceedings of ASME FEDSM'01-18030*, ASME New Orleans, May 2001

[37] ISHIBASHI, M., TAKAMOTO, M. Discharge coefficient of superaccurate critical nozzle accompanied with the boundary layer transition measured by reference super-accurate critical nozzles connected in series. *Proceedings of ASME FEDSM'01-18036*, ASME New Orleans, May 2001

Discharge coefficients for cylindrical throat Venturi nozzles

[38] GRENIER, P. Discharge coefficients of cylindrical nozzles used in sonic conditions. *NEL fluid Mechanics Silver Jubilee Conference, Paper No. 1.2.* East Kilbride, Glasgow: National Engineering Laboratory, November 1979

[39] PEIGNELIN, G. and BENZONI, A. Utilisation des Venturi tuyères fonctionnant en régime d'écoulement sonique comme étalons de débits de gaz sous pression. *Note dc Gaz de France, no 67842,* 1967

[40] PEIGNELIN, G. and GRENIER, P. Etude du coefficient de décharge des tuyères fonctionnant en regime d'ecoulement sonique au col utilisées comme étalon pour le mesurage de débit de gaz sous pression. *Congrès de l'Association technique du gaz en France,* 1978

[41] GRENIER, P. Etude statistique du coefficient de décharge des tuyères a col cylindrique fonctionnant en régime sonique. *Note du Gaz de France, n°81474,* August 1981

[42] SPENCER, E. A., EUJEN, E., DIJSTELBERGEN, H.H. and PEIGNELIN, G. Intercomparison campaign on high pressure gas flow test facilities. *EEC Document No. EW 6662.* Brussels-Luxembourg: ECSC-EEC-EAEC, 1980

[43] BOSIO, J., CABROL, J.F., KEREVAN, P. Intercomparison of the calibration results obtained at Gaz de France Alforville and K-Lab on a critical flow Venturi nozzle. *FLOMEL'94*. Glasgow, Scotland

[44] VULOVIC, F. Report on the intercomparison carried out on eight European benches using a sonic nozzle as transfer standard. *EUROMET PROJECT No. 307*. - M.CERMAP VUL/SZ 97/I/129, 1997

[45] VULOVIC, F., VINCENDEAU, E., VALLET, J.P., WINDENBERGER, C., VILLANGER, O., BOSIO, J. Influence of the thermodynamics calculations on the flow-rate of sonic nozzles. *Int. Fluid Flow Measurement Symposium*, Denver 27-30 June, 1999

Other references

[46] IAPWS Formulation 1995 for the Thermodynamic Properties of Ordinary Water Substance for General and Scientific Use. IAPWS, 1996

[47] STEWART, D.G., WATSON, J.T.R. and VAIDYA, A.M. The effect of using atmospheric air in critical flow nozzles. *Paper presented at the 4th International* Symposium *on Fluid Flow Measurement*, Denver, June 1999

ICS 17.120.10

Price based on 38 pages